

Quantification of Mass Fraction of
Organic Mass Functional Groups:
Fourier Transform Infrared spectroscopy
(FTIR) Application for Mobile Sources
Testing

Report to the
California Air Resources Board
Contract 13-322

Prepared by:
Lynn M. Russell and Elizabeth Koch Singh

Scripps Institution of Oceanography
University of California at San Diego
9500 Gilman Drive, La Jolla CA 92093-0221

20 June 2016

DISCLAIMER

This report was prepared by the University of California, San Diego (Contractor) as an account of work sponsored by the California Air Resources Board (CARB), under contract 13-322. The statements and conclusions in this report are those of the contractor, and not necessarily of CARB. The mention of any commercial products, their use in conjunction with material reported here, or their source is not to be construed as an actual or implied endorsement of such products.

ACKNOWLEDGEMENTS

We thank the CMU-UCB research team for their cooperation and contribution to this report. Particularly we acknowledge Professors Allen Robinson at Carnegie Mellon University and Allen Goldstein at UC Berkeley and their group members for organizing the El Monte experiments. We also thank Yunliang Zhao, Georges Saliba, Greg Drozd, Rawad Saleh, Jun Liu, Kylee Chang, and Fabian Hagen for contributing to sample collection and supplemental analyses.

We thank Dr. Nehzat Motallebi for her management and advice of this CARB contract, as well as Hector Maldonado for his leading role in organizing the El Monte mobile source testing.

Table of Contents

List of Tables.....	iv
List of Figures	v
List of Acronyms.....	vi
Abstract	1
Executive Summary.....	2
1. Introduction	4
1.1 Background and Motivation	4
1.2 Research Objectives	9
2. Filter Collection during Vehicle Testing	11
2.1 Analysis Methods	11
2.2 Vehicles and Test Conditions	14
3. FTIR Analysis and Results Summary.....	22
3.1 FTIR Spectra of Filters	22
3.2 FTIR Organic Mass and OFG Composition	32
Overview of Results	32
Organic Mass by Vehicle Category.....	34
Organic Functional Group Composition.....	36
Comparison of FTIR OC with EGA OC for CVS Samples	42
Comparison of FTIR OM with AMS OA for PAM and SMOG Chamber Samples	44
4. Comparisons of Vehicle Emissions to Atmospheric Sampling and Chamber Experiments.....	50
4.1 Comparisons to Atmospheric Sampling	50
4.2 Comparisons to SOA Chamber Experiments.....	52
5. Distribution of Results	54
6. Conclusions and Findings	55
6.1 Primary Conclusions	55
6.2 Research Highlights	56
References	59

List of Tables

Table 1. Organic mass and functional group composition for individual vehicle samples by CVS, PAM (lights on), and SMOG filters.

Table 2. Range (upper line) and average with standard deviation (lower line) of organic mass measured by FTIR in the emissions by car type (in $\mu\text{g m}^{-3}$).

Table 3. Range of organic mass measured in the emissions by car type in mg/kg-fuel.

Table 4. Mass fraction of organic functional groups for CVS samples by vehicle category.

Table 5. Mass fraction of organic functional groups for PAM (lights on).

Table 6. Mass fraction of organic functional groups for SMOG chamber samples.

List of Figures

Figure 1. FTIR spectra of PZEV, SULEV, and ULEV samples for CVS, PAM, SMOG and blanks, with specific test vehicles given in the legend. X-axis is wavenumber; Y-axis shows absorbance, held constant by row, with blank values shown at more than 15 times less than CVS, PAM or SMOG for comparison.

Figure 2. FTIR spectra of LEV2, LEV1, pre-LEV samples for CVS, PAM, SMOG and blanks, with specific test vehicles given in the legend. X-axis is wavenumber; Y-axis shows absorbance, held constant by row, with blank values shown at more than 5 times less than CVS, PAM or SMOG for comparison.

Figure 3. Example FTIR spectrum and curve-fitting analysis of an atmospheric fine particle sample collected in Mexico City, in which alcohol, aromatic, alkene, alkane, carbonyl, and amine functional groups are quantified by characteristic absorption peaks. (Illustration of algorithm discussed in [Liu *et al.*, 2009].)

Figure 4. Pie graphs for each vehicle emissions category of average FTIR functional group contributors for CVS, PAM-On, and SMOG. Colors indicate alkane (blue), amine (orange), organic hydroxyl (hot pink), carboxylic acid (green), nonacid carbonyl (teal), and groups below detection (gray).

Figure 5. FTIR functional group composition by sampled air concentration for CVS, PAM-On, and SMOG by individual vehicle in $\mu\text{g m}^{-3}$.

Figure 6. FTIR functional group composition as emission factors for CVS, PAM-On, and SMOG by car type in mg/kg-fuel.

Figure 7. Comparison of organic carbon measured by ARB EGA versus organic carbon measured by FTIR in $\mu\text{g m}^{-3}$ for the CVS samples.

Figure 8. Comparison of AMS OA with FTIR OM for PAM (lights on) chamber samples. The line fit has a slope of 0.69 with a correlation $R^2 = 0.57$. (AMS measurements were provided by CMU on 1/5/16.)

Figure 9. Comparison of AMS and FTIR measurements of OM during SMOG chamber sampling at the times noted. Note that the concentration varied during SMOG chamber sampling and FTIR and AMS measurements did not coincide. (AMS measurements were provided by CMU on 1/5/16.)

List of Acronyms

AMS	Aerosol Mass Spectrometer
CARB	California Air Resources Board
CCN	Cloud Condensation Nuclei
CE	Collection Efficiency
CVS	Constant Volume Sampler
DPF	Diesel Particulate Filter
EC	Elemental Carbon
EGA	Evolved Gas Analysis
FTIR	Fourier Transform Infrared
GDI	Gasoline Direct Injection
LEV	Low Emission Vehicle
LEV1	LEV vehicles certified during 1994-2003
LEV2	LEV vehicles certified during 2004-2012
NR-PM ₁	Non-refractory PM ₁
OA	Organic Aerosol
OC	Organic Carbon
OFG	Organic Functional Group
OM	Organic Mass
PAM	Potential Aerosol Mass
PFI	Port Fuel Injection
PM ₁	Submicron Particle Mass
PM _{2.5}	Fine (<2.5 micron diameter) Particle Mass
PMF	Positive Matrix Factorization
Pre-LEV	Pre-LEV, i.e. vehicles certified prior to 1994
PSA	Possible Sampling Anomaly
PZEV	Partial Zero Emission Vehicle
SOA	Secondary Organic Aerosol
SMOG	Mobile Photochemical Reaction Chamber
SULEV	Super Ultra-Low Emission Vehicle
TOA	Thermal-Optical Absorbance
TOR	Thermal-Optical Reflectance
ULEV	Ultra-Low Emission Vehicle
VOC	Volatile Organic Compound

Abstract

Fourier Transform Infrared (FTIR) spectroscopy of organic mass collected on Teflon filters sampled from primary and secondary vehicle emissions were used to characterize the amount and organic functional group (OFG) composition of non-volatile organic mass (OM). FTIR has been used for ambient air measurements in numerous past atmospheric sampling studies (including CalNex 2010 field study at Bakersfield to quantify organic mass functional groups as part of ARB funded research project "Improved characterization of primary and secondary carbonaceous particles, Final Report for ARB 09-328"). However, this project was the first use of FTIR for vehicle emissions testing that involved engine source and reacted-chamber engine emission sampling. These engine studies may provide a way to separate chemically the gas and diesel contributions to ambient POA and SOA. The FTIR characterization of chemical functionality allows both reduced artifacts for organic carbon quantification and separation of POA and SOA, providing different organic signatures with specific vehicular sources. The vehicle emission classes included in the study met the following emission standard categories: Partial Zero Emissions Vehicle (PZEV), Super-Ultra-Low-Emission Vehicle (SULEV), Ultra-Low-Emission Vehicle (ULEV), Pre-Low Emission Vehicles (LEV) (prior to 1994), LEV1 (1994-2003), and LEV2 (2004-2012). Vehicle emission categories showed differences in amount and composition of emissions, with low primary OM concentrations and emission factors characterizing the newer vehicle categories (PZEV, ULEV, SULEV). For all vehicle emission categories, we found the OFG composition was clearly distinguished for primary and secondary samples: primary emissions (sampled by a Constant Volume Sampler, CVS) had alkane and amine groups but no oxidized groups; secondary OM was approximately half oxidized groups with one-third alcohol and two-thirds acid groups in the Potential Aerosol Mass (PAM) chamber and more than two-thirds oxidized groups (mostly acid) in the mobile photochemical (SMOG) chamber. Comparing the compositions measured by this vehicle testing with atmospheric sampling reveals that PAM and SMOG chamber samples are very similar to vehicle-related emission factors identified in Bakersfield and elsewhere. The low OM in CVS samples is consistent with their small contribution to atmospheric sampling, and their amine group fraction indicates that vehicle emissions provide primary amine groups in the non-volatile fraction of primary emissions. Comparisons to FTIR OFG composition from laboratory smog experiments with individual hydrocarbon pre-cursors indicate that the PAM and SMOG chamber samples collected here are similar to the secondary OM composition produced by very high oxidant exposures of both aromatic and alkane pre-cursors.

Executive Summary

Introduction: Atmospheric aerosols can affect the radiative balance of the Earth, reduce air quality, and adversely impact human health. However, quantitative evaluation of these effects is uncertain. To improve our understanding of the properties of aerosol particles, we need to know more about their chemical composition and sources. The composition of the organic fraction of aerosols is poorly characterized. By improving our understanding of the amount and composition of OM from vehicular sources, this project will improve our understanding of organic aerosols.

Background: Source apportionment of organic carbon (OC) and mass (OM) has identified both primary and secondary contributions from the modern vehicular fleet. However, quantifying and characterizing those contributions is limited both by the limited chemical characterization of past emission measurements and by the lack of new vehicle models in past studies. FTIR has been used for ambient air measurements in numerous past atmospheric sampling studies (including CalNex 2010 field study at Bakersfield to quantify organic mass functional groups as part of ARB funded research project "Improved characterization of primary and secondary carbonaceous particles, Final Report for ARB 09-328"). However, this project was the first use of FTIR for vehicle emissions testing that involved engine source and reacted-chamber engine emission sampling. These engine studies may provide a way to separate chemically the gas and diesel contributions to ambient POA and SOA. The FTIR characterization of chemical functionality allows both reduced artifacts for organic carbon quantification and separation of POA and SOA, providing different organic signatures with specific vehicular sources. The vehicle emission classes included in the study met the following emission standard categories: Partial Zero Emissions Vehicle (PZEV), Super-Ultra-Low-Emission Vehicle (SULEV), Ultra-Low-Emission Vehicle (ULEV), Pre-Low Emission Vehicles (LEV) (prior to 1994), LEV1 (1994-2003), and LEV2 (2004-2012).

Methods: Fourier Transform Infrared (FTIR) spectroscopy of organic mass collected on Teflon filters sampled from primary and secondary vehicle emissions was used to characterize the amount and organic functional group (OFG) composition of non-volatile organic mass (OM). FTIR spectroscopy was used to quantify the mass concentrations of OFG, including alkane, alcohol (hydroxyl), carboxylic acid, amine, and carbonyl groups. The masses of all OFG measured were summed to give the non-volatile OM. Samples were collected of primary emissions using a Constant Volume Sampler (CVS); secondary OM was collected from the Potential Aerosol Mass (PAM) chamber and from the mobile photochemical (SMOG) chamber.

Conclusions: For all vehicle emission categories, we found the OFG composition was clearly distinguished for primary and secondary samples:

primary emissions (sampled by CVS) had alkane and amine groups but no oxidized groups; secondary OM was approximately half oxidized groups with one-third alcohol and two-thirds acid groups in the PAM chamber and more than two-thirds oxidized groups (mostly acid) in the SMOG chamber. Comparing the compositions measured by this vehicle testing with atmospheric sampling reveals that PAM and SMOG chamber samples are very similar to vehicle-related emission factors identified in Bakersfield and elsewhere. The low OM in CVS samples is consistent with their small contribution to atmospheric sampling, and their amine group fraction indicates that vehicle emissions provide primary amine groups in the non-volatile fraction of primary emissions. Comparisons to FTIR OFG composition from laboratory smog experiments with individual hydrocarbon pre-cursors indicate that the PAM and SMOG chamber samples collected here are similar to the secondary OM composition produced by very high oxidant exposures of both aromatic and alkane pre-cursors. These results indicate that future research on further application of FTIR measurements for vehicle sources testing could improve both the quality and the specificity of their quantification of particle emissions.

1. Introduction

Carbonaceous compounds can constitute the largest fraction of fine particulate matter (PM_{2.5}) in many regions, but their composition is usually the least understood [Jimenez et al., 2009; NRC, 1996]. In addition, aerosol particles play an important role in the radiative balance of the atmosphere, with their organic fraction representing one of the largest uncertainties in our ability to quantify climate cooling and feedback effects. The organic fraction of particles constitutes a significant fraction of particles transported in the troposphere across North America and the Arctic, making important contributions to light scattering and health impacts. After sulfates, organic compounds are the most abundant component of fine aerosol globally and are thought to comprise 10-50% of the mass of fine aerosol. The quantity and composition of the man-made contribution to atmospheric organic particles are not well characterized. This study addresses this knowledge gap by providing better characterization of organic carbon in order to improve ARB's ability to track organic functional groups in particles from sources that reduce air quality and harm health.

1.1 Background and Motivation

The organic fraction of atmospheric particles is comprised of a complex mixture of hundreds or thousands of individual compounds [Hamilton et al., 2004], which originate from a variety of sources and processes. In urban areas, the major source is fossil fuel combustion from gasoline- and diesel-powered vehicles and

other industrial activities (e.g., oil burning). Emissions from these sources are largely composed of alkane and aromatic hydrocarbons, with a minor fraction of alkene compounds [Kirchstetter *et al.*, 1999; Schauer *et al.*, 1999]. After emission, VOCs are transported from their sources during which time they are oxidized in the atmosphere, forming low-volatility products that can condense into the particle phase. The organic aerosols formed in the atmosphere are categorized as “secondary organic aerosol” (SOA) as opposed to “primary organic aerosol” (POA), organic aerosols directly emitted at their sources.

Better understanding and characterization of carbonaceous aerosols through improved measurements are needed in order to identify their emission sources and their impacts on health and visibility. Because the organic fraction of carbonaceous aerosol has contributions from multiple sources, there is a need for improving the linkages between sources and this fraction of ambient PM concentrations. Since volatile organic carbon (VOC) emissions can produce organic PM_{2.5} by forming SOA, measurements of sources and ambient aerosol are needed to investigate the discrepancies between emission inventories and atmospheric measurements.

Since organic aerosol is the largest contributor to both aerosol air quality and radiative forcing in many parts of the Earth, assessing their atmospheric role requires observations of organic functional groups. The data collected will also increase our knowledge of organic aerosol in regions where there are currently

only sparse data. Identifying organic functional groups helps us to understand their sources as well as their thermodynamic, microphysical, and optical properties. One example is that these properties determine the underlying processes that control particle-cloud interactions [Petters *et al.*, 2016]. These fundamental processes control the atmospheric chemistry of the indirect effect of particles on clouds, yet they are poorly understood. Preliminary calculations show that this indirect effect may be significant [IPCC, 2007]. Without acquiring detailed information on the chemical, hygroscopic, and optical properties as proposed in this study, a more accurate determination of the aerosol indirect effect is not possible.

Fourier Transform Infrared (FTIR) spectroscopy classifies organic compounds by their chemical functionality and provides a compromise between bulk organic carbon measurements and specific speciation techniques [Russell, 2003; Russell *et al.*, 2009b]. Organic compounds are reduced to functional groups and carbon chains, which provide a systematic approach to characterization. In this way, FTIR provides both the amount of oxidized carbon bonds and the chemical functional type of those bonds. Aerosol Mass Spectrometer (AMS) techniques provide mass spectrometric information about carbon-containing fragments and provide quantitative accuracy for OM of $\pm 20\%$ (similar to FTIR), although with quite different sampling limitations. This complementarity means that combining these two sets of complementary measurements provides a more complete picture of OM in particles than any single instrument, even though both

instruments can also be used separately to provide characteristic organic signatures for source identification.

As part of numerous past campaigns, the Russell group has collected fine particle mass on Teflon filters for quantification of organic functional group concentrations (FTIR) and elemental concentrations (XRF) [Day *et al.*, 2010; Frossard, 2011; Gilardoni *et al.*, 2007; Gilardoni *et al.*, 2009; Hawkins and Russell, 2010b; Hawkins *et al.*, 2010; Liu *et al.*, 2012; Maria *et al.*, 2002; Maria *et al.*, 2003; Russell *et al.*, 2009b; Russell *et al.*, 2010]. These techniques allowed not only for quantitative characterization of the organic composition of fine aerosol, but also identification of source categories and quantitative source contributions through the use of elemental tracers and positive matrix factorization (PMF). In many cases, the sample collection was conducted alongside simultaneous AMS measurements, allowing for comparison of total organic mass and providing complementary information on organic composition (mass fragments as opposed to chemical functional groups).

Comparisons between FTIR OC and Evolved Gas Analysis (EGA) OC were carried out for several field projects [Maria *et al.*, 2003; Gilardoni *et al.*, 2007; Bates *et al.*, 2012; Hayes *et al.*, 2013], resulting in good agreement (+/-20%) with correlations between 0.6 and 0.9 for ambient samples where the adsorption of SVOCs on quartz was small compared to the OM sampled.

FTIR and quadropole AMS OM were compared in detail by Russell et al. [2009a] for eight separate field projects around the world [Gilardoni et al., 2007; Russell et al., 2009b; 2010; Frossard et al., 2011; Liu et al., 2009; Day et al., 2010], resulting in mild correlations ($0.5 < r < 0.75$), with two exceptions for the Scripps pier in summer (2008) with a slightly weaker correlation ($r = 0.51$) and for the Scripps pier in winter (2009) and TexAQS with slightly stronger correlations ($r = 0.83$ and $r=0.79$, respectively). For campaigns dominated by small, water or organic-containing particles, the AMS technique reports up to 40% more OM than quantified by FTIR absorption, after corrections to account for the AMS collection efficiencies are applied. Such discrepancies are within the conservative 20-30% uncertainties of each technique and suggest that losses of OM due to both volatilization in sample collection and omission of organic groups not resolved by FTIR or AMS are typically less than 20% [Russell et al., 2009b]. Larger discrepancies in which FTIR exceeds AMS occur in campaigns with larger concentrations of dust or other non-refractory particles (such as VOCALS where the linear slope is 0.38), as these solid particles may not be efficiently sampled by the AMS (even though they can serve as a condensational sink for a significant fraction of the organic mass).

Further comparisons between FTIR and high resolution AMS have been discussed by Liu et al. [2012], Bates et al. [2012], Frossard et al. [2014], Corrigan et al. [2013], and Hayes et al. [2013], among others. Similar to the earlier comparisons, correlations (r) varied between 0.6 and 0.9 and magnitudes were

within the conservative 20-30% uncertainties of each technique. Frossard et al. [2014] showed that marine particles are under-counted by the AMS since they are largely refractory, consistent with expectations. Liu et al. [2012] suggested that urban emissions may be under-counted by FTIR due to the higher contribution of SVOCs, especially for fresh, high-concentration vehicle emissions.

1.2 Research Objectives

The objective of this study is to quantify the mass fraction of organic functional groups (including those formed as SOA) to particle-phase emissions from vehicular combustion. The research also improves the characterization and quantification of organic particles by including measurements and comparisons of OM composition using Fourier Transform Infrared (FTIR) spectroscopy. This work is essential for addressing the following open and important questions:

- How much ambient OA is POA and how much is SOA?
- Are chamber models representative of ambient SOA?
- Are engine tests representative of ambient POA?

For these reasons, the FTIR signature is essential both for interpreting existing and future ambient OM measurements and for establishing the relevance of chamber/engine tests to California's atmosphere. Since the Russell group already has ambient air measurements (from CalNex and other studies, e.g. *Liu et al. [2012]*), this project only involves engine source and reacted-chamber engine emission sampling. The ability of FTIR to characterize the chemical

functionality of both POA and SOA organic carbon will allow us to associate different organic signatures with specific vehicular sources. Consequently these engine studies provide a very good way to separate vehicular contributions to ambient POA and SOA.

2. Filter Collection during Vehicle Testing

During the first months of the project, we prepared the filters for sample collection. Tailpipe emissions from on-road gasoline vehicles and their SOA production have been investigated during the dynamometer testing at the California Air Resources Board's (CARB) Haggen-Smit Laboratory from 11 May to 21 June 2014. The samples were transported to Scripps Institution of Oceanography for FTIR analysis. Initial samples were scanned during the first two weeks of testing for evaluation and review of the methods implemented; these tests showed that filter loadings included alkane group mass amounts above the limit of quantification.

The work involved planning and collaboration with ARB staff and with scientists Allen Robinson from Carnegie Mellon University (CMU) and Allen Goldstein University of California Berkeley (UCB), as well as their research groups. Through their support, we were also able to collect the proposed FTIR filters as well as additional samples for STXM-NEXAFS analysis.

2.1 Analysis Methods

The analysis methods proposed for sampling diluted and reacted tailpipe emissions are analogous to those used previously by the Russell group for ambient conditions [Day et al., 2010; Frossard, 2011; Gilardoni et al., 2007; Gilardoni et al., 2009; Hawkins and Russell, 2010b; Hawkins et al., 2010; Liu et

al., 2012; Maria et al., 2002; Maria et al., 2003; Russell et al., 2009b; Russell et al., 2010]. During the early stages of the campaign, FTIR filters were sent to Scripps Institution of Oceanography for analysis to ensure that the sampling protocols, collection intervals, and concentrations provided sufficient mass on filters to ensure that functional group concentrations are adequately above detection limits. For cleaner vehicles, the primary organic aerosol concentrations were lower than expected ($<2 \mu\text{g}/\text{m}^3$), but sufficient mass loading was available to quantify most of the major organic functional groups identified with our technique.

The aerosol samples were collected on Teflon filters, which were then frozen and transported back to the laboratory where they were scanned using FTIR spectroscopy in a humidity and temperature-regulated clean room (Class 100 equivalent). The FTIR analysis was performed in the Russell laboratory in Keck 224 and 228 at the Scripps Institution of Oceanography, which includes workspace for aerosol instrumentation development and calibration. The advanced FTIR spectrometer from Bruker Optics has been calibrated for direct aerosol transmission measurements on filters. The laboratory includes two recently renovated rooms with hoods and gas/water plumbing. The Class 100 equivalent clean room houses the Bruker FTIR spectrometer to minimize sample contamination before, during and after spectra are taken.

Teflon filters were used as substrates and showed negligible adsorption of volatile organic compounds (VOCs) on back filters collected downstream of selected sample filters [Maria et al., 2003; Gilardoni et al., 2007]. Blank filters provided a measure of adsorption during sampling and contamination during handling (loading and unloading) and storage. Organic components collected on back filters provide a measure of sampling error and were below detection.

Each Teflon filter was non-destructively analyzed by transmission FTIR. FTIR measurements of absorbance characterized the functional groups associated with major carbon bond types, including saturated aliphatic (alkane) groups, unsaturated aliphatic (alkene) groups, aromatic groups, alcohol (used here to include phenol and polyol) groups, carboxylic acid groups, non-acidic carbonyl groups, primary amine groups, organonitrate groups, and potential organosulfate groups. The spectra were interpreted using an automated algorithm [Russell et al., 2009b; Takahama et al., 2013] to perform baselining, peak-fitting, and integration based on the approach described previously [Maria et al., 2002; 2003; 2004; Maria and Russell, 2005], using calibrations revised for the Tensor 27 spectrometer with RT-DLATGS detector (Bruker Optics, Ettlingen, Germany) [Gilardoni et al., 2007]. Additional calibrations of amine groups and carboxylic acid groups were used to improve accuracy by quantifying additional peaks at 2625 cm^{-1} and $2600\text{-}2800\text{ cm}^{-1}$ [Russell et al., 2009b]. Complete sets of internal standards for organic components of the atmosphere are not available, in part because the particle composition of vehicle emissions is not fully known. In

addition, the complexity of mixtures of organic compounds in emissions results in mixtures that cannot be fully resolved by FTIR. All of the measured functional groups are summed to calculate organic mass (OM). Estimates of the accuracy, errors, and detection limits of this technique for ambient measurements are discussed in Russell [2003].

To complement the POA sampling of emissions, Dr. Russell's group used some of the filters for chamber samples of oxidized vehicle emissions to provide the composition of the two SOA proxies provided by CMU and Aerodyne Research Inc. (Aerodyne). Filters from both the Aerodyne Potential Aerosol Mass flow reactor (PAM) and the CMU SMOG chambers were collected and analyzed as allowed by scheduling and sampling limitations.

2.2 Vehicles and Test Conditions

The fleet tested in this study included 27 vehicles, which were mostly light duty gasoline vehicles (LDGV) certified to the ARB super ultra-low emission vehicle (SULEV) emissions standards as well as some ultra-low emission vehicles (ULEV) and partial zero emission vehicles (PZEV). The fleet also included a mix of older vehicles: LEV2 – low emission vehicles certified to the 2004-2014 light duty vehicle (LDV) standards, LEV1 – low emission vehicle certified to the 1994-2003 LDV standards, and several diesel vehicles. The LEV1 category included only Port Fuel Injection (PFI) engines. The SULEV category includes only Gasoline Direct Injection (GDI) engines. The PZEV and LEV2 categories

included both GDI and PFI gasoline engines. The ULEV category included both GDI and PFI gasoline engines, as well as two diesel vehicles, one with and one without a Diesel Particulate Filter (DPF).

The vehicles were tested as a function of 1) engine operating mode - cold start versus hot running, 2) engine technology type - gasoline direct injection versus port fuel injection (GDI vs PFI), and 3) vehicle age and mileage, i.e. new/low versus old/high. The gasoline vehicles were tested using the same commercial California 'summertime' fuel (E10).

The measurements included three types of sampling: Constant Volume Sampling (CVS) system, Potential Aerosol Mass (PAM, Aerodyne Research Inc., Billerica, MA), and a mobile photochemical SMOG chamber (Weitkamp 2007). The PAM chamber provides sampling continuously either with "lights on" or "lights off" at consistent conditions, similar to a continuous-flow reactor. The "lights off" mode provides a measure of primary OM in the absence of secondary contributions from photochemical products of VOCs. Due to the short sampling time and diluted concentrations the "lights off" samples all had concentrations similar to the blank levels, so CVS measurements are used instead as primary OM measurements.

The FTIR samples from the CVS during each vehicle test were collected by sampling the CVS air through a Teflon filter at 10 L/min with flows monitored by

mass flow meters. The Teflon filter was placed in a stainless steel filter holder and housed in a temperature controlled box (~47°C). For the UC cycle, the CVS air was not sampled during the 10-min hot soak. For other cycles, the CVS air was sampled through the entire test cycles.

The smog chamber experiments of dilute exhaust from gasoline vehicles were conducted using the CMU mobile chamber. This mobile chamber was a 7 m³ Teflon® bag suspended in a metal frame [Hennigan et al., 2011] and was located inside the test cell during this study. Before each experiment, the chamber was flushed overnight using clean air treated by silica gels, HEPA filters and activated charcoal in series and with UV lights (Model F40BL UVA, General Electric) turned on.

The dilute exhaust was drawn from the constant volume sampler (CVS) and injected into the chamber by a Dekati® diluter through silcosteel® stainless steel tubing. Both the diluter and transfer line were electrically heated and maintained at ~47°C, matching the CVS temperature. Eleven of these experiments were only filled during the period of the first UC bag. The rest of these experiments were filled through the entire UC, except for the 10-min hot-soak period. The NMHC emissions occur dominantly during the period of the first UC bag. The concentration of NMHCs in the chamber was approximately the same when the chamber was filled by the emissions during the first UC bag versus the entire UC, especially for experiments with SULEV vehicles. The two chamber experiments

that were sampled by FTIR were performed with the smog chamber filled by the entire UC, except for the 10-min hot-soak period.

Following the injection of the dilute exhaust, the ammonium sulfate seed particles were created by a constant-output atomizer (TSI, model 3075) and passed through a diffusion dryer and a neutralizer before injecting into the chamber. The seed particles reduced the induction time of SOA formation and were used to determine the particle wall losses during each experiment. Nitrous acid (HONO) was used as a hydroxyl radical (OH) source and added into the chamber by bubbling clean air through a solution prepared by mixing 0.1 M NaNO₂ and 0.05 M H₂SO₄ with a volume ratio of 1:2. A known amount of butanol-*d*₉ (Cambridge Isotope Laboratories, MA) was added to determine the OH concentration. Propene was also added to adjust the NMHC-to-NO_x ratio (ppb C/ppb NO_x) to match a typical urban level of ~3:1 ppbC/ppb NO_x [Gordon *et al.*, 2014]. After all gases and particles have been injected and mixed, the UV lights were switched on to initiate the photo-oxidation reactions.

Both particles and gases in the chamber were characterized by a suite of instruments. The particle number and volume in the chamber were measured using a scanning mobility particle sizer (SMPS, TSI classifier model 3080, CPC model 3772 or 3776). The nonrefractory submicron particle mass and chemical composition were measured by a high-resolution time-of-flight aerosol mass spectrometer (HR-AMS, Aerodyne, Inc., MA). CO₂ was measured by a LI-820

monitor (Li-Cor Biosciences, NE); NO_x , CO and O_3 was measured by API-Teledyne T200, T300 and 400A analyzers, respectively. The concentration of butanol- d_9 was measured by proton transfer reaction-mass spectrometry (Ionicon, Austria). The NMHC concentration in the chamber was not measured. However, the initial NMHC concentration in the chamber was calculated based on the NMHC concentration measured inside the CVS and the dilution factor determined by dividing the CO_2 concentration measured in the CVS by the one in the chamber. The dilution factor determined by CO_2 was confirmed by measurements of CO and NO_x in the CVS and chamber.

The particle and organic vapor wall losses were estimated in order to determine the SOA production. In the present study, the organic vapors were assumed to maintain equilibrium with both suspended and wall-bound particles [Gordon et al., 2014; Hildebrandt et al., 2009].

The PAM is an oxidation flow reactor. The average gas-phase species residence time in the PAM was approximately 100 s. Despite the short residence time, the PAM can produce high concentrations of oxidants that enable the simulation of atmospheric photo-oxidation on timescales from a day to several days [Kang et al., 2007; Lambe et al., 2011].

Unlike the smog chamber wherein OH radicals were produced by photolysis of HONO , OH radicals in the PAM were produced via O_2 , O_3 and H_2O

photochemistry [Li et al., 2015]. Four UV mercury lamps (BHK Inc.) were used to initiate photochemistry inside the PAM. The lamps emit light at 185 and 254 nm. At 185 nm, O_2 is photolyzed to produce O_3 , and H_2O is photolyzed to produce OH and HO_2 . At 254 nm, O_3 is photolyzed to produce O(1D), which reacts with H_2O to produce OH. O_3 levels inside the PAM (0– 20 ppm) are not expected to significantly influence SOA formation because SOA precursors present in vehicle emissions are dominated by aromatics and saturated hydrocarbons that are unreactive toward O_3 [May et al., 2014; Zhao et al., 2016]. High O_3 levels suppress reactions of nitric oxide (NO) with organic peroxy radicals (RO₂) formed from OH oxidation of vehicle emissions, but the effect on SOA formation is probably minor.

The OH exposure (the product of the OH concentration and average residence time in the PAM) for the PAM experiments in this study was set to be equivalent to 3-day atmospheric photo-oxidation processes at the OH concentration of 1.5×10^6 molecules cm^{-3} . The OH concentration was determined by measuring the decay of SO_2 as a function of lamp intensity in off-line calibration. The maximum SOA production from tailpipe emission would be determined under this OH exposure based on results from recent PAM experiments conducted in a traffic tunnel [Tkacik et al., 2014].

Two types of PAM experiments were conducted with UV lights on and with UV lights off, which were defined as “lights-on” experiments and “lights-off”

experiments for discussion. OM measured during the lights on experiments was the sum SOA formed from photo-oxidation of dilute exhaust and POA. In contrast, OM measured during lights-off experiments was only POA. Prior to each experiment, the PAM was flushed with clean air and with UV lights on to reduce the organics from the PAM walls. The clean air flow was turned off about 10 min before the vehicle testing; then, the CVS air was drawn through the PAM to determine the dynamic blank for the PAM experiment till the start of the vehicle testing.

During the vehicle testing, the dilute exhaust was drawn through the PAM directly from the CVS without further dilution. The sampling line from the CVS to the PAM was electrically heated and maintained at ~47°C. Both gases (CO, CO₂, NO_x, O₃) and particles out of the PAM were characterized using the same array of instruments for the smog chamber experiments. The sampling flow for these instruments was alternated between the smog chamber and the PAM through a three-way ball valve. NMHCs out of the PAM were not measured, but the concentration of NMHCs sampled into the PAM should be same as the one in the CVS because no dilution was made during the sampling of CVS air through the PAM.

The FTIR samples from the smog chamber and PAM were collected by sampling oxidized air through Teflon filters at 4 L/min and at room temperature. The sampling of the FTIR samples from the PAM started when the vehicle testing

started and continued through the entire test cycle. The FTIR samples from the smog chamber were collected when the photo-oxidation processes in the smog chamber were completed and the sampling lasted about an hour.

3. FTIR Analysis and Results Summary

3.1 FTIR Spectra of Filters

Fourier Transform Infrared (FTIR) spectroscopy classifies organic compounds by their chemical functionality and provides a compromise between bulk organic carbon measurements and specific speciation techniques [Russell, 2003; Russell et al., 2009b]. Quantified functional groups can include alkane, alcohol, amine, carbonyl, and carboxylic acid groups (alkene and aromatic groups are also quantified if present above 1-3% OM; organonitrate and organosulfate groups are quantified if present above 5-10% OM). Ratios of oxygen to carbon (O/C) and OM-to-OC can be calculated from FTIR analysis, revealing trends in oxidation and phase partitioning. Time series of FTIR spectra, organic functional group concentrations and OM/OC were completed within approximately one month following the sampling campaign.

The FTIR spectra for the CVS, PAM (lights on), and SMOG samples collected are shown in Figures 1 and 2. The blanks and PAM (lights off) are also included. The spectra show clearly that the FTIR signals exceed blank values for most of the samples.

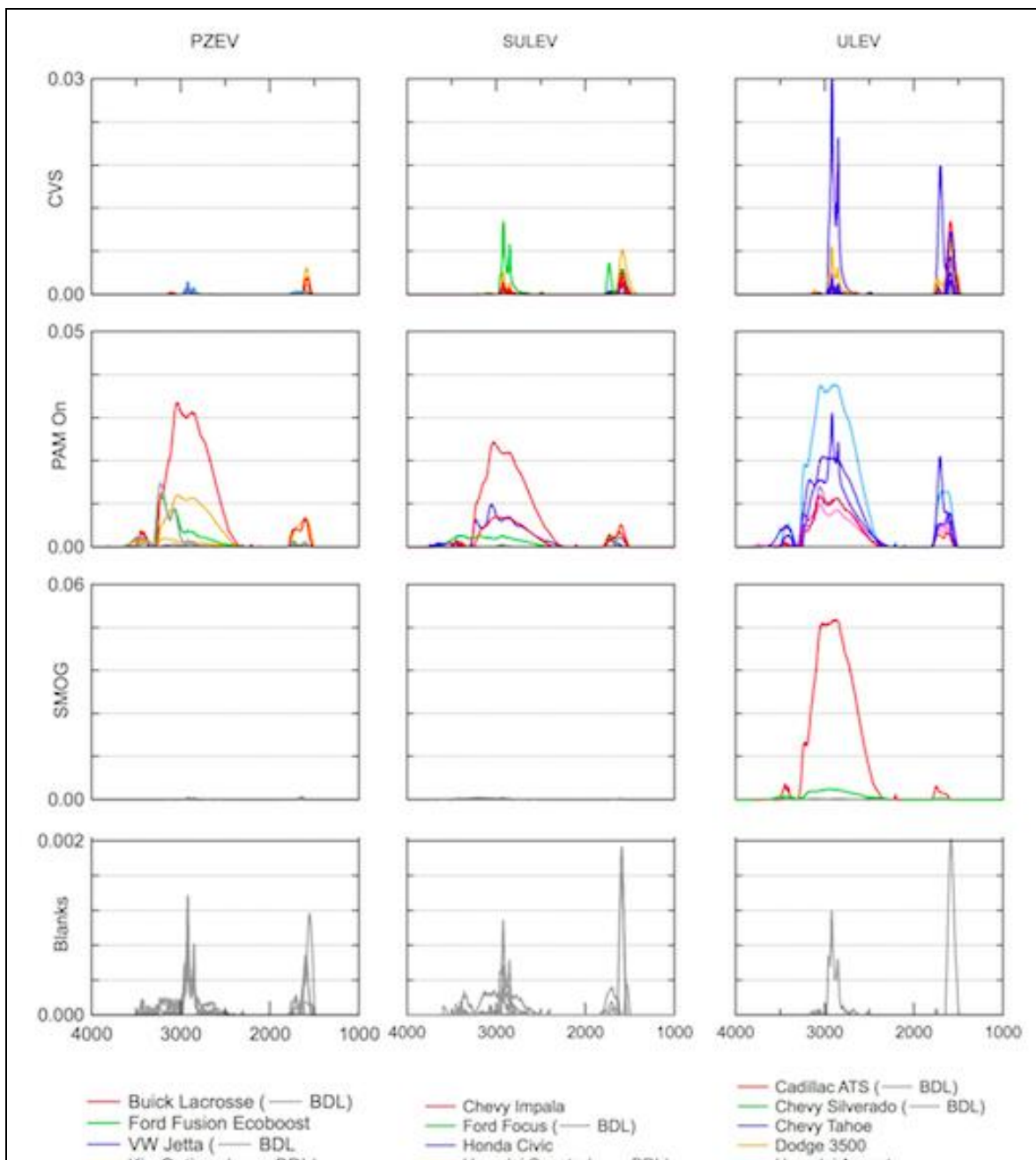
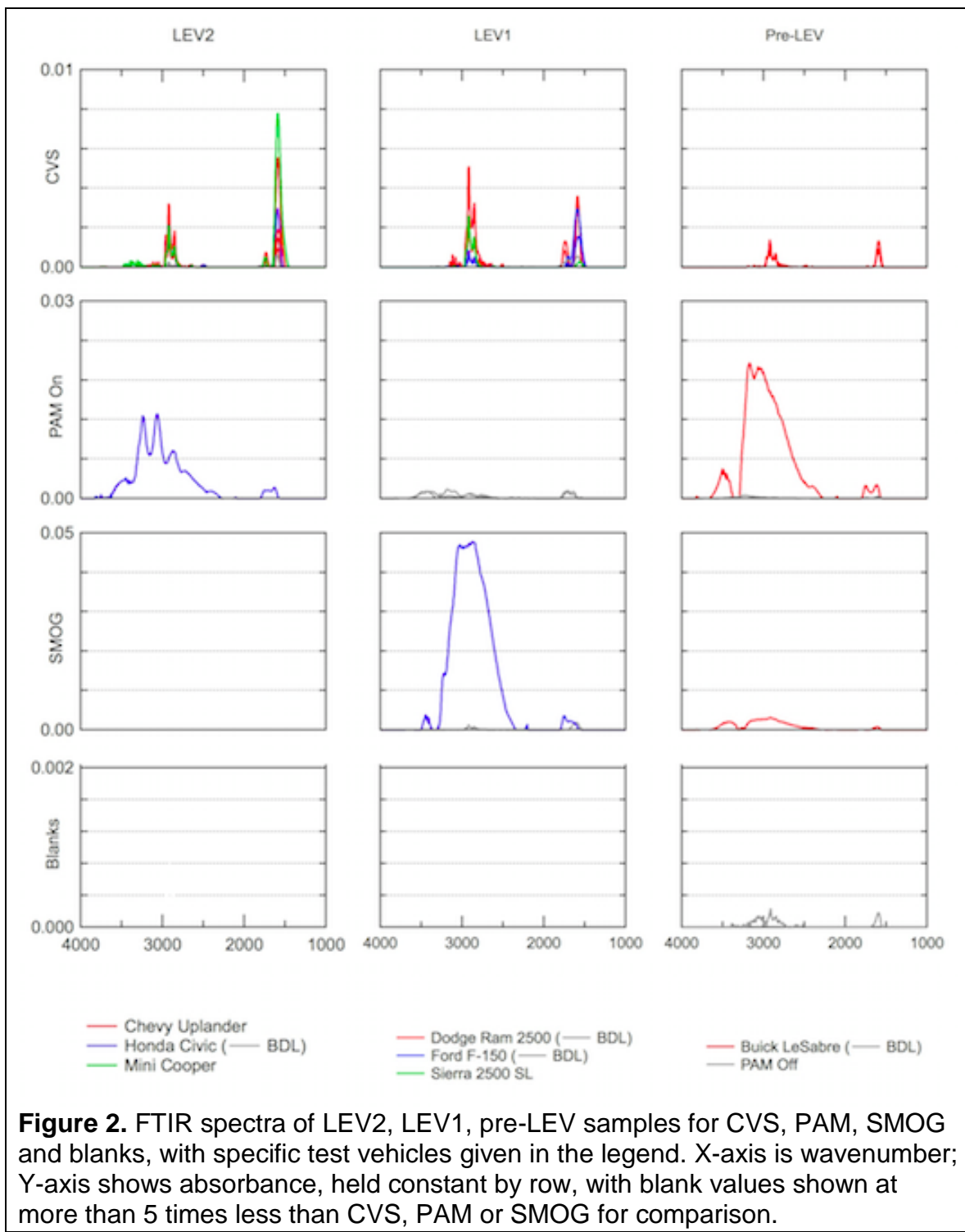


Figure 1. FTIR spectra of PZEV, SULEV, and ULEV samples for CVS, PAM, SMOG and blanks, with specific test vehicles given in the legend. X-axis is wavenumber; Y-axis shows absorbance, held constant by row, with blank values shown at more than 15 times less than CVS, PAM or SMOG for comparison.



To quantify organic functional groups in each spectra, an automated algorithm [Maria et al., 2002; Russell, 2003; Russell et al., 2009a] was used to baseline the spectra for the wavenumber range 4000-1500 cm^{-1} (which excludes the regions of Teflon absorption). The spectra were integrated for calibrated absorption peaks of major organic functional groups of organic molecules including aliphatic alkane groups, aliphatic alkene groups, organic hydroxyl (alcohol) groups, primary amine groups, aromatic groups, carboxylic acid groups, non-acid carbonyl groups, organonitrate groups, and organosulfate groups. Alkene, aromatic, and organosulfate groups were below detection for all samples collected in this project.

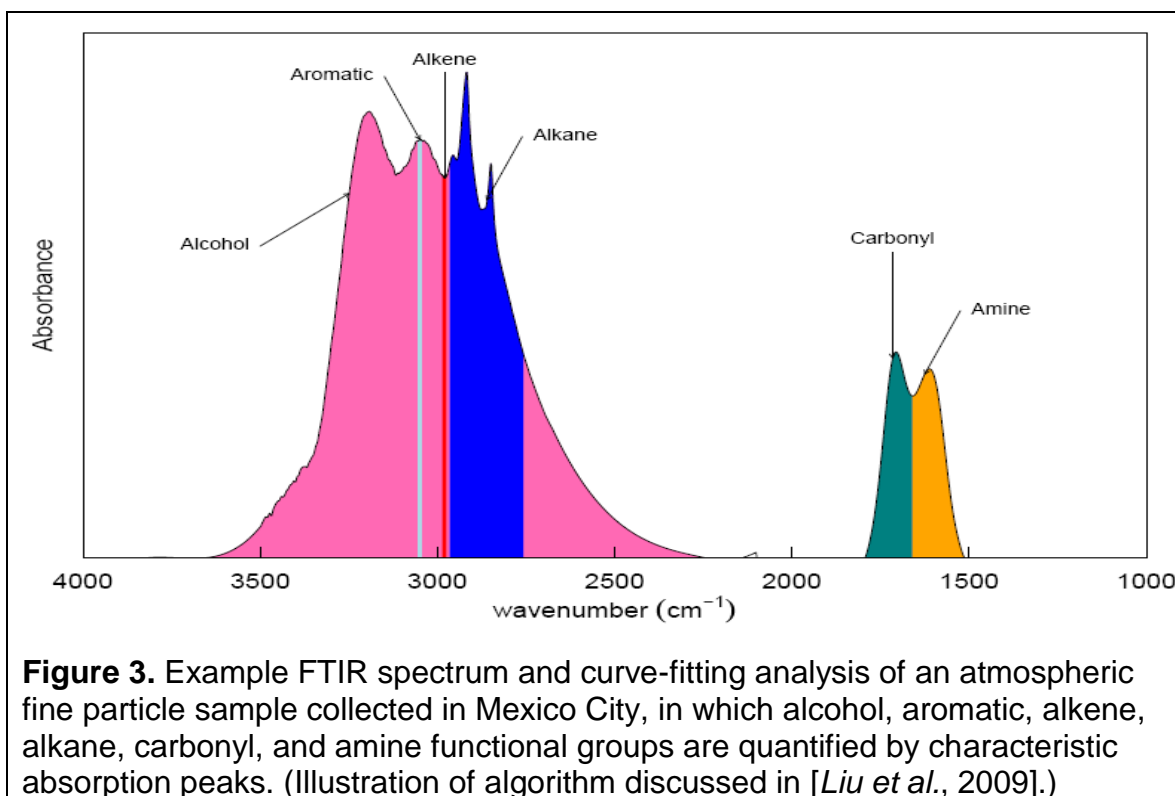


Figure 3 shows an example FTIR spectrum with the functional group peaks labeled after background subtraction and with fitted peaks. Functional groups measured by FTIR spectroscopy have been calibrated using organic compound standards with well-documented techniques [Maria et al., 2003; Russell et al., 2009a].

FTIR spectroscopy avoids the molecular mass conversion factors used in bulk organic carbon (OC) measurements (i.e. the use of an assumed OM/OC), which improves the ability to measure organic mass (OM) directly. Limits of quantification for FTIR spectroscopy and AMS spectrometry are typically within 20% of the organic mass, representing a significant improvement over traditional techniques such as evolved gas analysis (EGA) [Gilardoni et al., 2007; Gilardoni et al., 2009; Russell et al., 2009a], primarily due to the use of Teflon rather than quartz filters to minimize VOC-adsorption artifacts. Using FTIR-based measurements, the errors of determining organic mass are reduced to between 9 and 33%, with typical values of 21% for atmospheric sampling. Calibrations to laboratory-generated standards show that the scatter for a mass determination for a single known compound provides a standard deviation of less than 3% [Maria et al., 2002; Russell, 2003]. For ambient sampling, we have found that less than 5% of OM is from groups that are not detected because they are below detection limit. Estimates of the accuracy, errors, and detection limits of this technique for ambient measurements are discussed by Russell [2003].

Specifically for measuring vehicle emissions, additional uncertainty considerations are needed. OM has non-linear relationships with dilution especially at very low concentrations. Hence, both the chemical composition and the concentration of the emissions can vary with dilution in ways that do not simply scale with the dilution ratio. Further, the chemical composition and the concentration of the exhaust can vary due to differences in the maintenance of the vehicles, after treatment technologies employed, and the driving cycle (and during each phases of the driving cycle). Dr. Russell obtained from ARB information on the dilution ratios in the tunnel in order to calculate emission ratios. The ARB OC results will also be used for comparison to the FTIR-measured OC and OM concentrations.

Table 1 summarizes the organic mass and functional group composition for individual vehicle samples by CVS, PAM (lights on), and SMOG filters. Note that the values for Organic Mass (OM) are given in $\mu\text{g m}^{-3}$ (and mg/kg-fuel in parentheses). Colors indicate alkane groups (blue), amine groups (orange), acid groups (green), alcohol groups (pink), and groups below 5% (gray). (Organonitrate groups are not included as only one sample had more than 5%).

In Table 1, masses are reported as mass concentrations ($\mu\text{g m}^{-3}$) and emission ratios (mg/kg-fuel). Since sampling staff was limited, occasional problems with sample collection occurred. These samples are indicated in Table 1 by PSA (Possible Sampling Anomaly).

Table 1. Organic mass and functional group composition for individual vehicle samples by CVS, PAM (lights on), and SMOG filters. Masses are reported as $\mu\text{g m}^{-3}$ (and mg/kg-fuel).

Emissions Category	Vehicle	Test Date	Test Time	CVS		PAM On		SMOG		Blanks
				Organic Mass	Composition	Organic Mass	Composition	Organic Mass	Composition	
PZEV	Buick Lacrosse	06/04/14	AM1	6.1 (1.4)		120 (26.6)		0.04 (0.009)		
	Ford Fusion Eco Boost	05/20/14	PM1			5.77 (1.22)				
	VW Jetta	05/21/14	AM	1.2 (0.46)		4.1 (1.6)				
		05/22/14	PM2							0.47 (0.16)
		05/22/14	PM2							1.1 (0.37)
	KIA Optima	06/02/14	AM1	6.7 (1.9)		32.2 (9.13)		0.3 (0.1)		
		06/02/14	PM1	1.1 (0.16)		50.8 (7.85)				
		06/03/14	PM2	2.3 (0.53)						0.84 (0.19)
		06/13/14	AM1	0.45 (0.11)						
	Toyota Camry	05/22/14	AM1			1.39 (0.50)				0.46 (0.17)
		05/22/14	PM1	1.6 (0.49)		2.3 (0.68)				
		05/23/14	PM2	0.22 (0.080)						0.88 (0.32)
Non-PZEV	Chevy Impala	06/03/14	AM1	1.6 (0.28)		75.9 (13.2)				0.55 (0.096)
		06/04/14	PM2	1.2 (0.21)						2.5 (0.43)
		06/18/14	AM1	7.4 (1.3)		31.9 (5.73)				
		05/16/14	PM1			0.3 (0.07)				

Table 1 (continued). Organic mass and functional group composition for individual vehicle samples by CVS, PAM (lights on), and SMOG filters. Masses are reported as $\mu\text{g m}^{-3}$ (and mg/kg-fuel).

Emissions Category	Vehicle	Test Date	Test Time	CVS		PAM On		SMOG		Blanks Organic Mass
				Organic Mass	Composition	Organic Mass	Composition	Organic Mass	Composition	
SULEV	Ford Focus Titanium	5/16/14	PM2			8.75 (2.1)				1.5 (0.36)
		05/21/14	PM1	9.0 (1.5)		5.1 (0.83)				
	Honda Civic Hybrid	06/03/14	PM1	1.4 (0.47)		20.7 (6.8)				
		06/05/14	PM2	1.1 (0.38)						0.81 (0.28)
	Hyundai Sonata	05/20/14	AM	4.4 (0.95)						
		05/21/14	PM2	0.30 (0.065)						
		05/23/14	PM1	6.6 (0.89)				3.6 (0.49)		
	Mercedes C350	05/19/14	PM1	1.4 (0.29)				0.4 (0.08)		
		05/20/14	PM2	1.2 (0.24)						
Non-SULEV	Cadillac ATS	06/11/14	AM1	3.7 (0.71)				34 (6.6)		
		06/11/14	PM1	0.31 (0.041)						
		06/12/14	PM2	1.1 (0.23)						
		06/19/14	PM1	5.9 (1.2)		28.3 (5.63)				
	Chevy Silverado	06/05/14	PM1	1.6 (0.29)						
		06/16/14	PM1	0.24 (0.046)				6.3 (1.2)		12 (2.2)
		05/29/14	PM1	53 (6.9)		95.1 (12.4)				

Table 1 (continued). Organic mass and functional group composition for individual vehicle samples by CVS, PAM (lights on), and SMOG filters. Masses are reported as $\mu\text{g m}^{-3}$ (and mg/kg-fuel).

Emissions Category	Vehicle	Test Date	Test Time	CVS		PAM On		SMOG		Blanks
				Organic Mass	Composition	Organic Mass	Composition	Organic Mass	Composition	
ULEV	Chevy Tahoe	06/12/14	AM1	1.8 (0.23)						
		06/12/14	PM1	1.3 (0.11)						
		06/17/14	PM1	17 (2.2)		55.4 (7.14)				
		06/18/14	PM1	6.7 (0.89)						
	Dodge Ram 3500	06/06/14	AM1	4.5 (0.73) PSA						
		06/06/14	PM1	2.7 (0.33) PSA						
		06/09/14	PM2	8.7 (1.1)						
	Hyundai Accent	05/27/14	PM2			159 (44.8)				
		05/28/14	PM2	3.5 (1.0)						
	Mazda 3	05/30/14	PM1	2.3 (0.62)		21.8 (5.91)				
	Nissan Juke	05/28/14	AM1	4.7 (1.2)		48.8 (11.9)		0.4 (0.08)		
		06/02/14	PM2	7.9 (1.9)						3.0 (0.73)
		06/17/14	AM1	5.2 (1.3)						
	Chevy Uplander	05/27/14	PM1	5.5 (0.88)						
		05/28/14	PM1	3.6 (0.58)						
		05/29/14	AM1	2.1 (0.33)						

Table 1 (continued). Organic mass and functional group composition for individual vehicle samples by CVS, PAM (lights on), and SMOG filters. Masses are reported as $\mu\text{g m}^{-3}$ (and mg/kg-fuel).

Emissions Category	Vehicle	Test Date	Test Time	CVS		PAM On		SMOG		Blanks
				Organic Mass	Composition	Organic Mass	Composition	Organic Mass	Composition	
LEV2		05/29/14	PM2	1.6 (0.25)						
		05/30/14	AM1	9.8 (2.4)						
	Honda Civic CNG	06/18/14	PM2	0.75 (0.25)						
			AM1	0.39 (0.13)		33.2 (10.9)				
LEV1	Dodge Ram 2500	06/05/14	AM1	12 (2.4) PSA				0.93 (0.19)		
		06/09/14	PM1	3.4 (0.51) PSA						
	Ford F-150	06/04/14	PM1	0.0						
		06/06/14	PM2	1.0 (0.078)						
		06/09/14	AM1	0.56 (0.12)		1.9 (0.38)		22 (4.6)		
		06/10/14	PM2	1.1 (0.22)		1.7 (0.37)				
		Sierra 2500 SL	06/13/14	PM1	3.6 (0.46)					
	Pre-LEV	Buick LeSabre	06/10/14	AM1	1.6 (0.29)		64.7 (11.7)		8.6 (1.6)	
			06/10/14	PM1	3.2 (0.33)		0.33 (0.034)			
			06/11/14	PM2	1.0 (0.19)					0.27 (0.05)

3.2 FTIR Organic Mass and OFG Composition

The results from this project include comparisons of FTIR spectra, as well as calculation of organic functional groups, OM, OC, and associated uncertainties. Quantitative results have been integrated from spectra and used to evaluate the blank values and detection limits.

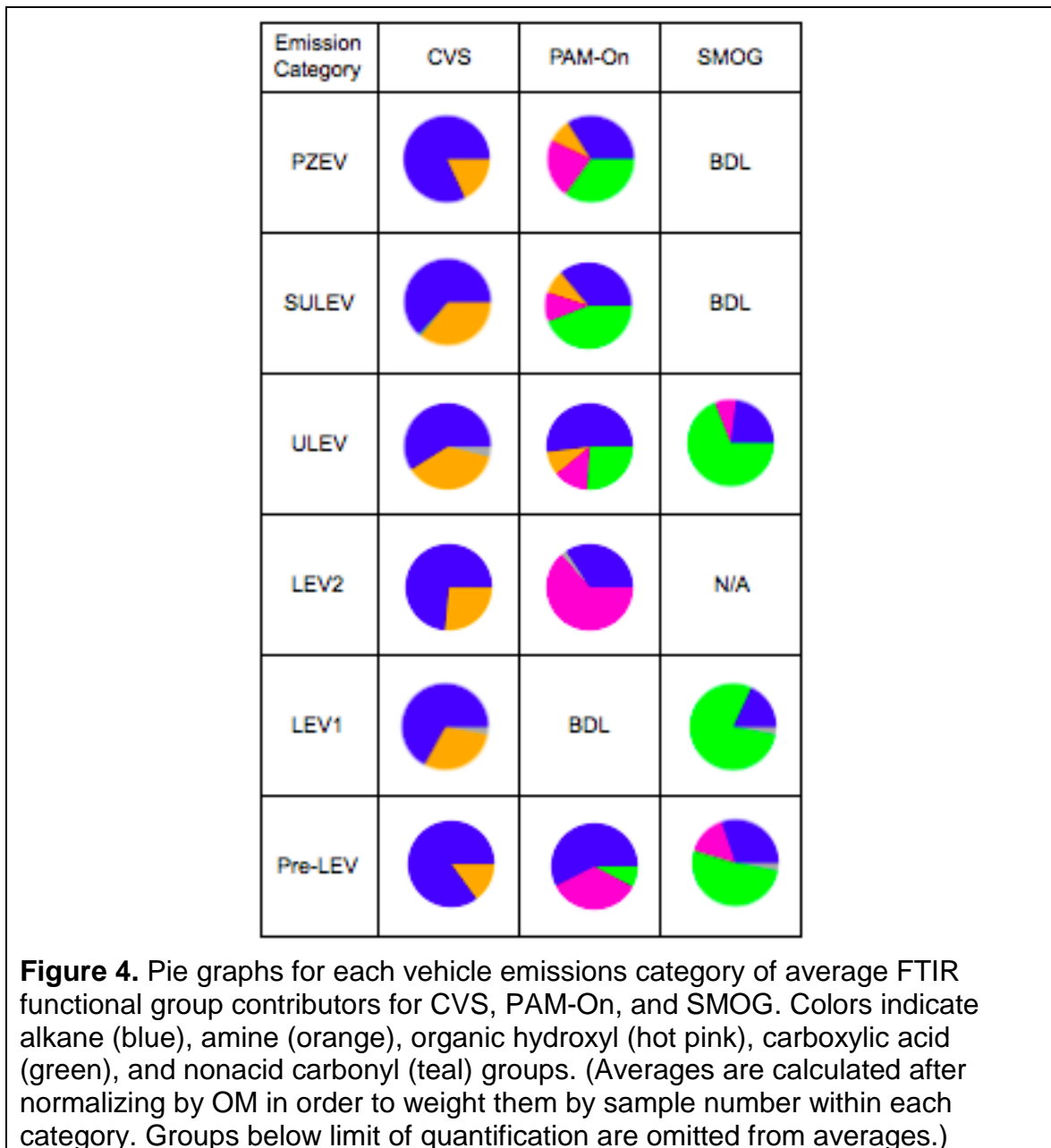
Overview of Results

As shown in Table 1 and summarized in Figure 4, the composition of almost all CVS samples included more than 50% alkane groups and a small but variable fraction of amine groups ($26\% \pm 25\%$). The variations in the amine group fraction are likely due to the influence of differing compositions of the intake air.

Note that group concentrations are quantitative but do not provide information on molecular composition. For example, alkane groups (C-H) are found in almost all organic molecules, so the fraction of alkane molecules is expected to be substantially less than the fraction of alkane groups. A few vehicles had higher amine group fractions. Most samples had OM concentrations of $0\text{-}4 \mu\text{g m}^{-3}$.

Concentrations of secondary particles measured in the PAM and smog chambers showed the presence of more oxidized functional groups (alcohol and carboxylic acid groups) groups in varying amounts. Two types of compositions were found for the PAM results: (1) the composition of “lights off” PAM being very similar to CVS, and (2) the “lights on” PAM were highly oxidized and had negligible alkane

or amine groups. For the smog chamber, five samples produced measurable SOA, which contained very high fractions of carboxylic acid functional groups with smaller fractions of alkane groups and alcohol groups.



Organic Mass by Vehicle Category

The results were analyzed by emission category to identify the differences in composition that are associated with different vehicle emission categories. These results show that individual vehicles have some similarities in POA based on vehicle type technologies. The new vehicle emission types that were tested as part of this project met the following vehicle standards: Partial Zero Emissions Vehicle (PZEV), Super-Ultra-Low-Emission Vehicle (SULEV), and Ultra-Low-Emission Vehicle (ULEV). The remaining vehicles are categorized by their model years: Pre-Low Emission Vehicles (LEV) (prior to 1994), LEV1 (1994-2003) and LEV2 (2004-2012). The concentration of the emissions is summarized in Table 2.

Table 2. Range (upper line) and average with standard deviation (lower line) of organic mass measured by FTIR in the emissions by car type (in $\mu\text{g m}^{-3}$).

Emission Category	# of vehicles	CVS	PAM-On	SMOG
PZEV	5	1.2-6.1 3.6 ± 2.6	5.4-119 52 ± 49	BDL
SULEV	5	1.1-9.0 3.8 ± 3.1	5.1-75 33 ± 30	BDL
ULEV	7	1.1-53 5.2 ± 4.1	22-158 68 ± 51	6.3-34
LEV2	3	1.6-9.8 4.5 ± 3.3	33	N/A
LEV1	3	1.0-11.6 4.1 ± 4.4	BDL	22
Pre-LEV	1	1.0-3.2 1.9 ± 1.1	64	8.6

Most of the samples of POA from the CVS had concentrations between 1 and 10 $\mu\text{g m}^{-3}$. One sample of the Chevy Tahoe on 5/29/14 was much higher than the other samples taken at 53 $\mu\text{g m}^{-3}$; the conditions of this sample were considered anomalous and are not included in Table 2. The concentrations of PAM samples (with lights on) had a larger range than the CVS samples, varying from as low as 5 up to 158 $\mu\text{g m}^{-3}$. There was substantial variability within emission categories, but this variability was comparable to the variability expected for repeat testing of an individual car. Four of the SMOG chamber samples taken were above the detection limit. Two of the samples are under 10 $\mu\text{g m}^{-3}$ and the other two are over 20 $\mu\text{g m}^{-3}$.

To compare the OM on a basis of kilogram of fuel burned (mg/kg-fuel), the ambient concentrations were converted from concentration to emission ratio using the volume of air passed through the instruments and the measurement of fuel burned. These values are shown in Table 3.

Most of the emissions range from 0.2 to 2 mg/kg-fuel. (The exception is the Chevy Tahoe excluded from Table 2 as discussed). For comparison, Gordon et al. (2014) found ~160 mg/kg-fuel for the pre-LEV vehicles, ~20 mg/kg-fuel for LEV1, and ~5 mg/kg-fuel for LEV2.

Table 3. Range of organic mass measured in the emissions by car type in mg/kg-fuel.

Emission Category	# of vehicles	CVS	PAM On	SMOG
PZEV	5	0.46-1.9	1.1-26	BDL
SULEV	5	0.20-1.5	0.83-13	BDL
ULEV	7	0.11-6.9	5.6-45	1.2-6.6
LEV2	3	0.25-2.4	11	N/A
LEV1	3	0.08-2.4	BDL	4.6
Pre-LEV	1	0.19-0.33	12	1.6

As indicated by the numbers of vehicles listed in Tables 2 and 3, this characterization of vehicle classes is limited by the small number of vehicles tested. In such a small sample, a single influential (and possibly atypical) vehicle may represent the entire category. Further study would be needed to characterize the fleet-appropriate average and distribution of compositions and concentrations for each vehicle class, in order to separately characterize lower and higher emitting vehicles within each class.

Organic Functional Group Composition

The organic mass collected for each test was also identified by functional group contribution using Fourier Transform Infrared Spectroscopy (FTIR). The functional groups measured by the FTIR were alkane, carbonyl, amine, alcohol,

individual vehicles are shown in Figures 5 and 6 by sampled air concentration and carboxylic acid groups. The organic functional group compositions for individual vehicles are shown in Figures 5 and 6 by sampled air concentration and as emission factors, respectively.

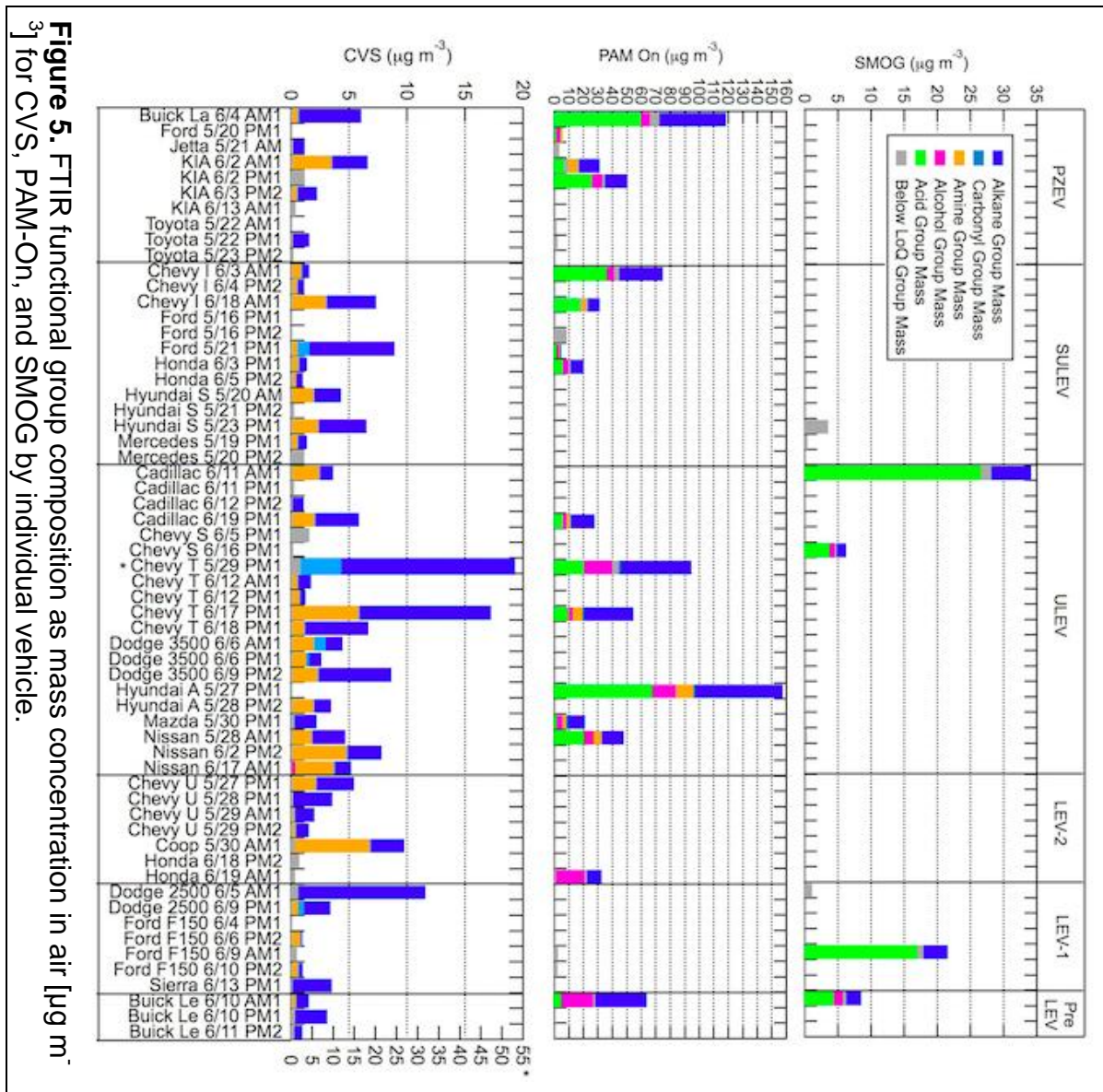


Figure 5. FTIR functional group composition as mass concentration in air [$\mu\text{g m}^{-3}$] for CVS, PAM-On, and SMOG by individual vehicle.

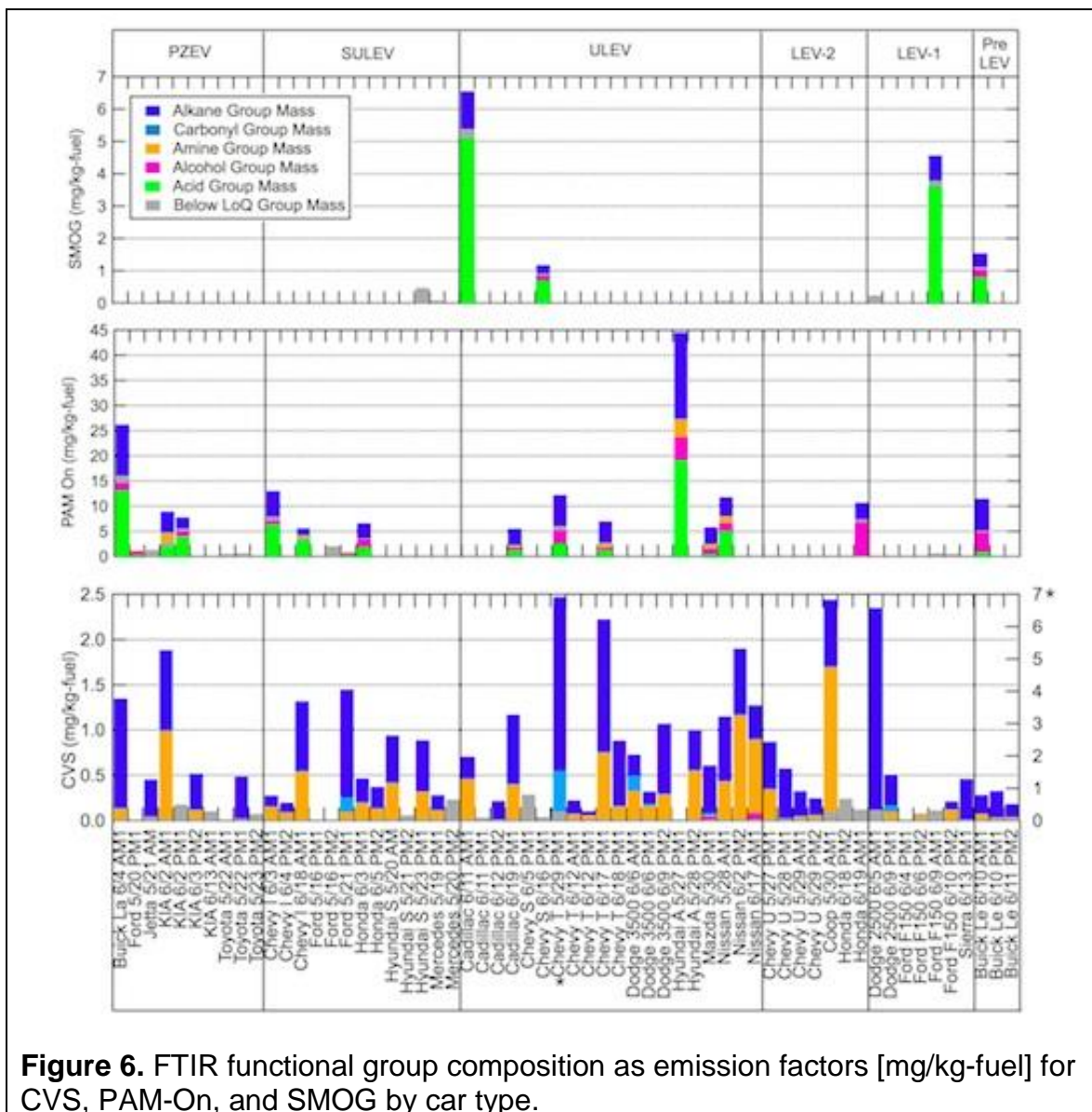


Table 4 summarizes the organic functional group composition for the CVS samples for each vehicle category. The mass fraction of alkane groups averaged between 60-85% of the total organic mass measured while the amine averaged between 15-40%. For almost all of the CVS samples, alcohol, carbonyl, and acid groups were below detection limit. The exception with the largest carbonyl group

was the Chevy Tahoe sample with anomalous sampling on 5/29/14 discussed above, which had less than 0.5 mg carbonyl group per kg fuel.

Table 4. Mass fraction of organic functional groups for CVS samples by vehicle category.

Emission Category	Alkane	Amine
PZEV	0.82 \pm 0.20	0.18 \pm 0.20
SULEV	0.63 \pm 0.09	0.36 \pm 0.12
ULEV	0.59 \pm 0.22	0.37 \pm 0.21
LEV2	0.72 \pm 0.27	0.26 \pm 0.26
LEV1	0.67 \pm 0.31	0.30 \pm 0.32
Pre-LEV	0.85 \pm 0.07	0.15 \pm 0.07

The fraction of alkane group in the PAM (lights on) samples is much lower than for the CVS samples – approximately 33-60%, as summarized in Table 5. The fraction of amine group detected also drops to approximately 10% or near detection. Most vehicles show much higher amounts of alcohol group and acid group with some samples measuring slightly more than half acid group. For almost all of the PAM samples, carbonyl groups were below detection limit.

To evaluate the background contamination in the PAM chamber, samples were also taken with the “lights off” in the PAM chamber. As expected, all of the PAM

(lights off) samples were below the instrument detection limit. Their composition is similar to the CVS samples with alkane group ranging from 65 to 90%, amine group approximately 5-35%, and trace amounts of alcohol group (likely from contamination in the chamber).

Table 5. Mass fraction of organic functional groups for PAM (lights on).

Emission Category	Alkane	Amine	Alcohol	Acid	Organonitrate
PZEV	0.34 \pm 0.15	0.08 \pm 0.08	0.2 \pm 0.2	0.35 \pm 0.18	0.02 \pm 0.03
SULEV	0.36 \pm 0.11	0.1 \pm 0.1	0.11 \pm 0.07	0.43 \pm 0.11	0.01 \pm 0.00
ULEV	0.52 \pm 0.13	0.09 \pm 0.03	0.13 \pm 0.06	0.26 \pm 0.14	0.01 \pm 0.00
LEV2	0.34	BDL	0.64	BDL	BDL
LEV1	BDL	BDL	BDL	BDL	BDL
Pre-LEV	0.57	BDL	0.35	0.08	BDL

Similar to the PAM measurements, little carbonyl or amine groups were measured for the SMOG samples, which are shown in Table 6. Much less alkane and alcohol groups were detected than for the PAM measurements. A much larger fraction of the OM was acid groups for the SMOG chamber samples than for the PAM (lights on) measurements. The higher acid fraction in the SMOG samples than the PAM samples is consistent with a higher O/C since acid groups have the highest O/C of the groups measured.

Table 6. Mass fraction of organic functional groups for SMOG chamber samples.

Emission Category	Alkane	Carbonyl	Amine	Alcohol	Acid
ULEV	0.19	0	0	BDL	0.78
ULEV	0.27	0	0	0.12	0.60
LEV1	0.18	0	0	BDL	0.78
Pre-LEV	0.30	0	BDL	0.15	0.51

Comparing the PAM and SMOG chambers, it is interesting to see that more oxidized OM was observed in chamber experiments. Likely this result is caused by the differences in oxidant exposure producing the observed differences in OFG. The PAM OH exposure was set to be 3-day equivalent oxidation under the atmospheric conditions [Yunliang Zhao, personal communication 1/22/16]. In contrast, the oxidation during chamber experiments was less than one day under the atmospheric conditions [Yunliang Zhao, personal communication 1/22/16]. The differences in carboxylic acid and hydroxyl groups between PAM and SMOG measurements are likely due to the lower OM concentration in the SMOG chamber reactions, which allows occurrence of multiple generations of oxidation of gas-phase organics before partitioning onto particles.

Comparison of FTIR OC with EGA OC for CVS Samples

The ARB also measured OC for the CVS by a specifically-calibrated protocol of evolved gas analysis (EGA, or heating the sample and measuring the gas that is evolved), in which the thermal-optical absorbance (TOA) method uses the IMPROVE_A temperature protocol with thermal-optical reflectance (TOR) for charring correction (California Air Resources Board, 2011c. SOP No. MLD139: Procedure for Organic Carbon and Elemental Carbon (OC/EC) Analysis of Vehicular Exhaust Particulate Matter (PM) on Quartz Filters [WWW Document]. URL. http://www.arb.ca.gov/testmeth/slb/sop139v1_1.pdf). For short, we refer to these results by the generic term “EGA” to distinguish them from the FTIR measurements. These results can be used for comparison to the FTIR-measured OC concentrations. This complementary approach to particle mass quantification provides a useful comparison, shown in Figure 7.

EGA was performed by standard methods for both bare quartz filters and quartz behind Teflon filters. The bare quartz filters include both particle-phase OC and substantial contributions from adsorbed VOCs, whereas the samples after the Teflon filters only contain adsorbed VOCs. A combined total of 66 tests were completed on the 24 vehicles. Of those 66 samples only 22 had a total organic carbon collected on quartz that was higher than the total organic carbon collected on the quartz behind the teflon. Of these 22, ten CVS samples had EGA OC above the variability of the tunnel blank ($10 \mu\text{g m}^{-3}$). Of the simultaneous 10 FTIR samples, two FTIR filters were omitted due to sampling anomalies and one FTIR

filter was below the detection limit of the instrument. The remaining seven measurements show a strong correlation between the organic carbon measured by the FTIR and the ARB instruments.

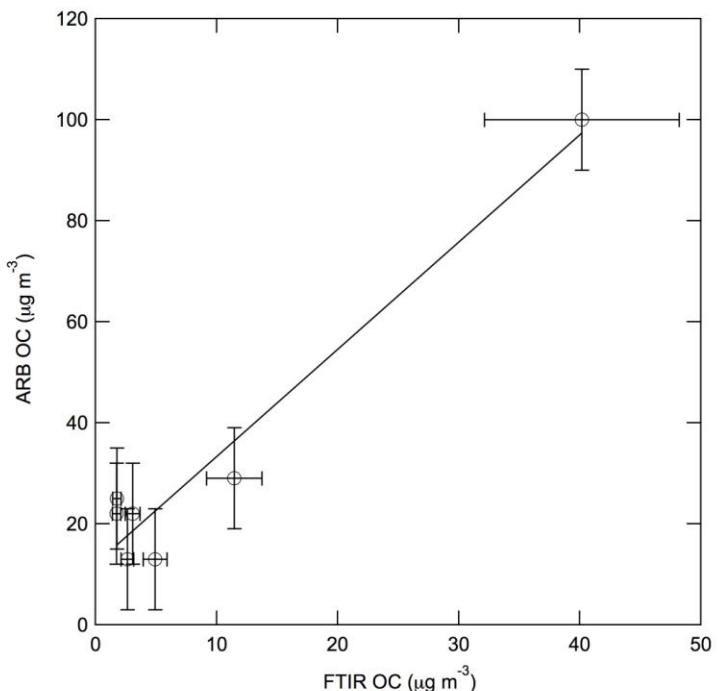


Figure 7. Comparison of organic carbon measured by ARB EGA versus organic carbon measured by FTIR in $\mu\text{g m}^{-3}$ for the CVS samples.

The FTIR OC are lower than the seven available EGA OC samples by a factor of approximately 2. Since the EGA samples were corrected for a large adsorbed vapor contribution, their uncertainty is comparable to or greater than the background measurements of $10 \mu\text{g m}^{-3}$. However, lower values of FTIR OC are also consistent with loss of SVOC from the Teflon filters used for collection. While ambient samples typically show such losses are less than 10% [Russell et al.,

2010], these primary vehicle emission samples might have higher contributions from SVOC that are preferentially lost more from the Teflon filters than from the quartz filters. This result is consistent with the FTIR Teflon filters efficiently collecting only the non-volatile OM and not adsorbing semi-volatile compounds.

Comparison of FTIR OM with AMS OA for PAM and SMOG Chamber Samples

CMU, Aerodyne, and UCB collected AMS OA measurements from the PAM and SMOG chamber samples. The available OA measurements were provided by CMU on 1/10/16 with CE=1.

Operation of the PAM chamber included a flow-through mode with no photochemical reactions (lights off) to provide a baseline for measuring pre-reaction composition. The identical setup was also operated with photochemical reactions (lights on) in order to characterize production of secondary organic products. Operation of the SMOG chambers included a collection phase to fill the chamber Teflon bag with diluted emissions and then a photochemical reaction phase during which the bag was sealed and lights were turned on. Products were monitored in real-time and by collection of filter samples for both chambers.

For the PAM (lights on) samples, Figure 8 shows that the limited number of available measurements for the same vehicle tests (13 samples) have a moderate correlation ($R^2 = 0.57$) with a slope of 0.69, within the $\pm 20\%$ uncertainty of both AMS and FTIR. While the higher OM from FTIR compared to AMS is within the stated instrument uncertainty, the on-average lower values of

the AMS could result either from using CE=1 or from adsorption of SVOCs onto the FTIR OM already collected on the filter. The short sampling times for these filters makes this unlikely at typical, slowly-varying atmospheric concentrations where the particles and vapors are at equilibrium. However, the high concentrations and fast reactions in the PAM chamber could result in rapid concentration changes and non-equilibrium conditions that might increase adsorption. Further measurements would be needed to rule out a contribution from this effect.

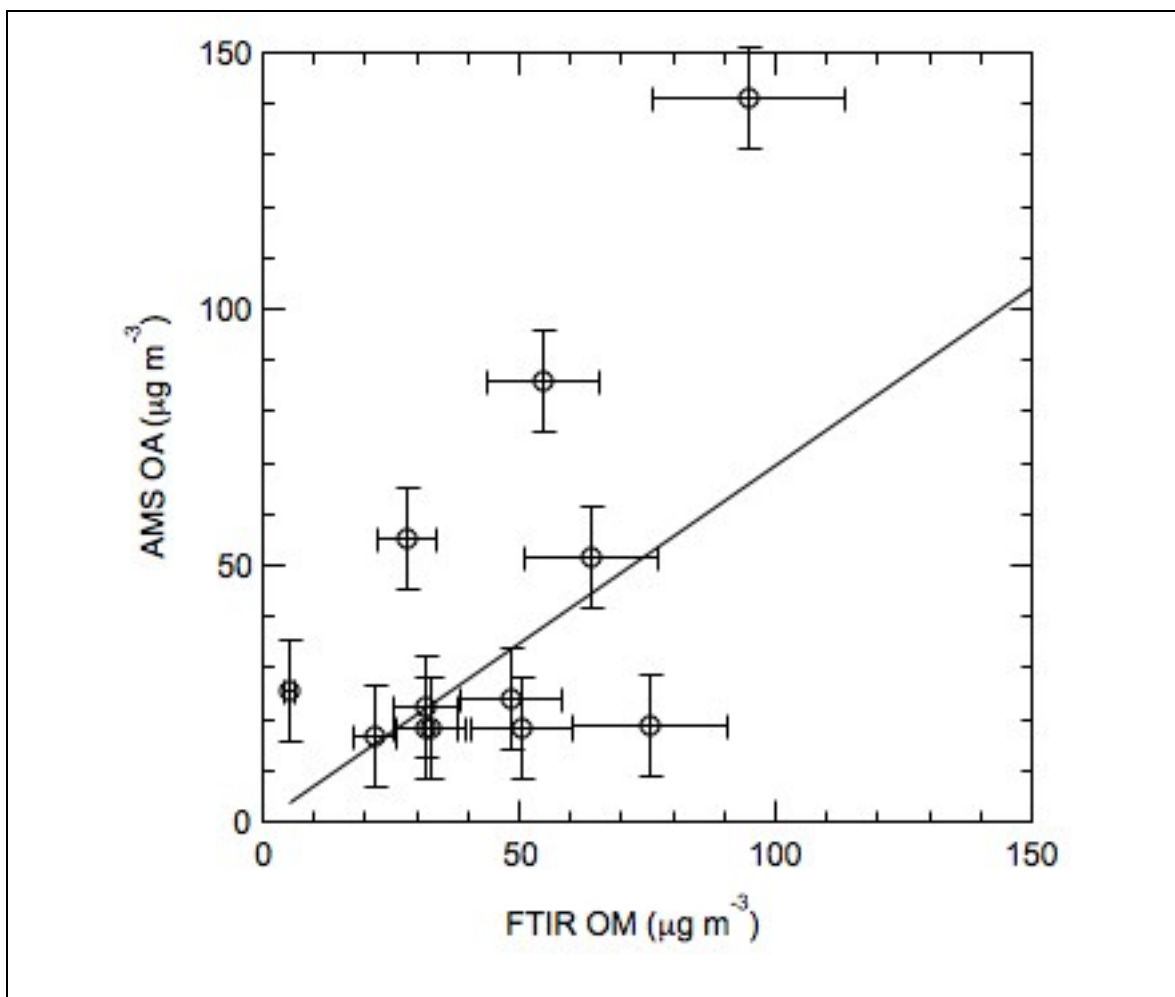


Figure 8. Comparison of AMS OA with FTIR OM for PAM (lights on) chamber samples. The line fit (forced to the origin) has a slope of 0.69 with a correlation $R^2 = 0.57$. (AMS measurements were provided by CMU on 1/5/16.)

There are two available AMS OA measurements for the SMOG chamber samples. Due to sampling limitations, the FTIR and AMS measurements could not be taken simultaneously, so the variation in organic particle mass concentration during time in the SMOG chamber means that the samples are not expected to be directly comparable. Figure 9 shows that the samples are generally consistent with higher concentrations for the Ford F150 (6/9) than for the Buick Le Sabre (6/10), even though the different sampling times appear to coincide with different chamber OM concentrations.

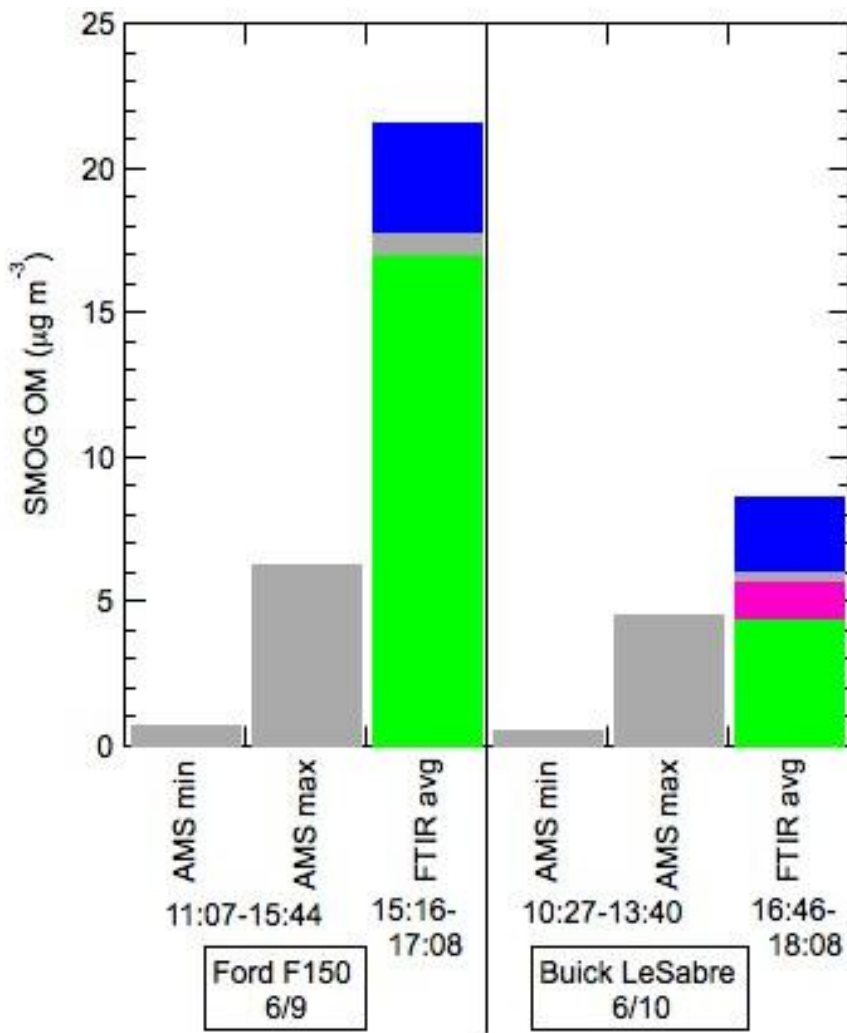


Figure 9. Comparison of AMS and FTIR measurements of OM during SMOG chamber sampling at the times noted. Note that the concentration varied during SMOG chamber sampling and FTIR and AMS measurements did not coincide. (AMS measurements were provided by CMU on 1/5/16.)

It is worth noting that, for an AMS CE=1, the FTIR OM is higher than the AMS for both PAM and SMOG chamber samples even though FTIR OC was lower than EGA OC for CVS samples. This higher apparent collection efficiency for FTIR is likely the result of the Teflon filters collecting non-volatile OM efficiently but losing some of the SVOC that may be captured by the quartz filters used for EGA. It is

also worth noting that a more typical value of CE=0.5 would make the FTIR OM and AMS OA more comparable for the SMOG chamber samples.

The PAM experiments were conducted with much more concentrated exhaust compared to the SMOG chamber experiments. During PAM experiments the exhaust was directly sampled from the CVS. During the smog chamber experiment exhaust was also drawn from the CVS, but it was further diluted through a Dekati® diluter and with clean air inside the SMOG chamber. Therefore, the concentrations of primary emissions, both NMHCs and POA inside the PAM reactor were greater (by a factor of 17 to 270) than those in the SMOG chamber. The substantially higher concentrations of NMHCs and OA favor the condensation of semi-volatile organic compounds formed from the oxidation NMHCs and subsequently prevent these compounds from further gas-phase oxidation to form lower volatility organic compounds. According to partitioning theory, semivolatile compounds with effective saturation concentrations 10 times higher would partition into the condensed phase during the PAM experiments compared to the chamber experiments. This difference in the saturation concentration is consistent with the addition of a hydroxyl functional group (an alcohol group) versus a carboxylic acid functional group into a compound [Kroll et al., 2008]. Meanwhile, the high OA concentrations favor the partitioning of primary semi-volatile organic compounds in particles over evaporation.

In addition to different concentrations of NMHCs and OA, the OH exposure (calculated by the OH concentration multiplied by the residence time) inside the PAM reactor was much larger. It was set to be equivalent to 3-day atmospheric oxidation at the OH concentration of 1.5×10^6 molecules cm^{-3} . In contrast, the OH exposure during the SMOG chamber experiment is less than 14 hours. The high OH exposure inside the PAM reactor oxidizes NO_x quickly to HNO_3 , which forms ammonium nitrate in presence of ammonia. High concentrations of ammonium nitrate in particles were observed during the PAM experiments in this field campaign. The formation of ammonium nitrate increases the particle surface area, which also favors the condensation of semi-volatile organic compounds compared to gas-phase oxidation.

In general, partitioning of semivolatile compounds to the condensed phase likely results in the OM being less oxidized than during the smog chamber experiments. Additional data analysis is ongoing for a comprehensive comparison between PAM and SMOG experiments for SOA formation based on measurements conducted as part of other contracts.

4. Comparisons of Vehicle Emissions to Atmospheric Sampling and Chamber Experiments

Our analyses also included evaluation of the CVS, PAM, and SMOG chamber compositions with prior measurements from chambers and atmospheric sampling. These comparisons are possible because, as part of numerous past campaigns, we have collected fine particle mass on Teflon filters for quantification of organic functional group concentrations (FTIR) and elemental concentrations (XRF) [Day et al., 2010; Frossard, 2011; Gilardoni et al., 2007; Gilardoni et al., 2009; Hawkins and Russell, 2010b; Hawkins et al., 2010; Liu et al., 2012; Maria et al., 2002; Maria et al., 2003; Russell et al., 2009b; Russell et al., 2010]. These measurements allowed not only for quantitative characterization of the organic composition of fine aerosol, but also identification of source categories and quantitative source contributions through the use of elemental tracers and positive matrix factorization (PMF). In many cases, the sample collection was conducted alongside simultaneous AMS measurements, allowing for comparison of total organic mass and providing complementary information on organic composition (mass fragments as opposed to chemical functional groups).

4.1 Comparisons to Atmospheric Sampling

One clear example of comprehensive ambient air measurements collected during previous studies is the Bakersfield measurements during CalNex 2010. The major functional groups found by Liu et al. [2012] in the organic mass collected at

Bakersfield include alkane (35%), hydroxyl (22%), and carboxylic acid (21%) groups. Much of the alkane and amine groups are associated with aromatic- or alkane-derived SOA was found to be from fossil fuel combustion associated with vehicles.

The CVS measurements from the vehicle emissions tested here were primarily alkane groups with a variable contribution of amine groups, similar to the fossil fuel combustion factors summarized in Table 1 of Russell et al. [2011]. FTIR spectra (Figures 1 and 2) for most CVS samples showed a double-peak in the alkane region and a clear single peak in the primary amine region. This structure is most similar to the Nighttime OFG factor in Bakersfield (Figure 6(a) in Liu et al. [2012]). In the daytime SOA factors measured at Bakersfield in summer, these peaks are rarely evident, and instead the spectra are overwhelmed by alcohol, acid, and carbonyl groups that have broader absorption regions. This result is consistent with unreacted POA remaining in the aerosol only during the colder nighttime temperatures, with a very small contribution from POA in the daytime Bakersfield FTIR samples.

The PAM and SMOG chamber samples had much smaller amounts of amine groups and larger fractions of alcohol and acid groups. The PAM chamber samples with lights on for the newer vehicles are the most similar to ambient samples with alkane groups averaging 35-50%, alcohol groups 10-20% and acid groups 25-45%. The older vehicles (Pre-LEV, LEV1, LEV2) have a smaller

fraction of acid groups and the SMOG samples have a higher fraction of acid groups than the ambient samples. The higher acid group fractions in the ULEV, SULEV, and PZEV are more similar to the OM factor from the Bakersfield study [Liu et al., 2012] that was associated with secondary products of vehicle emissions and correlated with gas-phase alkane compound contractions.

4.2 Comparisons to SOA Chamber Experiments

Comparisons of the PAM and SMOG chamber sample FTIR spectra to controlled, single-compound chamber studies show that the broad absorption region between 2500 and 3500 wavenumbers of the PZEV, SULEV, and ULEV PAM chamber samples are quite similar to toluene in a continuous flow chamber with excess oxidant [L.M. Russell, unpublished results from EPA chamber studies]. This result is expected since PAM chambers are designed with excess oxidant in order to maximize reaction of the hydrocarbons, similar to continuous flow chamber designs.

Batch-type reaction chambers for alkane and aromatic precursors typically result in more identifiable alcohol and acid group peaks as well as some unreacted alkane groups. The FTIR spectra from the SMOG chamber samples did not have much alkane group absorption, meaning that there was no evidence of unreacted alkanes remaining when the filters were collected. In part, this might be because the filter samples were collected near the end of the SMOG chamber

experiments. This sampling strategy was needed to optimize instrument collection times.

5. Distribution of Results

The results of this project were distributed by providing measurements and analyses to CARB and PIs Goldstein and Robinson. Preliminary results were shared during progress review meetings, including the 27 August 2015 progress review meeting. It is expected that these results will be used in publications describing the results of vehicle testing by the project leaders. Acknowledgement of these contributions will include co-authorship.

6. Conclusions and Findings

FTIR analysis provides the chemical functional group composition of primary and secondary vehicle emissions as well as organic mass reflective of the non-volatile fraction. Sample collection was carried out with minimal anomalous samples and within the bounds of the program constraints. Most samples were above detection for both OM and major OFG. The FTIR results show the accuracy expected and provide information not available from other techniques. Given the successful completion of these measurements, a number of conclusions are evident and are discussed below.

6.1 Primary Conclusions

Individual vehicles showed variable OM and compositions that were consistent with other studies. Vehicle emission categories showed some differences, with low primary OM characterizing the emissions of newer vehicles (0-2 mg/kg-fuel). Secondary OM were a factor of 10 or more larger for most vehicles. Clear differences in OFG composition were evident among the CVS, PAM, and SMOG samples, consistent with the differences expected between primary OM (negligible oxidized OFG) and secondary OM (50% or more oxidized OFG). Since the PAM and SMOG oxidation experiments were conducted under very different conditions, including different SOA precursor concentrations, particle concentrations, OH concentrations, residence times, and the VOC-to-NOx ratios, the different chemical compositions and concentrations of the products are not surprising.

These vehicle results support the interpretation of organic aerosol sources from Liu et al. [2012] and other studies. Similar organic functional group compositions were also seen in fuel combustion factors from a variety of other regions, summarized by Russell et al. [2010]. The direct correlation between FTIR and EGA OC measurements verifies that the measurements are comparable. These results indicate that future research on further application of FTIR measurements for vehicle sources testing could improve both the quality and the specificity of their quantification of particle emissions.

6.2 Research Highlights

1. Primary vehicle emissions sampled from CVS tests had very low OM concentrations and emission factors, with concentrations on average of 67% alkane and 31% amine functional groups.
 - a. Few other detectable functional groups were present with enough consistency for a clear determination given the variability in sampling conditions.
 - b. A couple samples showed carbonyl groups, notably the Chevy Tahoe on 5/29/14.
2. Secondary OM measured in the PAM and SMOG chambers showed much larger concentrations than the primary OM measured from the CVS, as well as the presence of oxidized functional groups (alcohol, carbonyl, and

carboxylic acid) in amounts that varied with the vehicle, as well as the sampling and reaction conditions. Generally, SMOG chamber samples showed more acid groups and fewer alcohol groups than PAM chamber samples, consistent with the longer reaction times at lower OM concentrations allowing for multiple generations of gas-phase VOCs before partitioning to particles.

- a. PAM chamber samples with lights on (set for 3-day equivalent oxidation) had an average of 42% alkane, 9% amine, 15% alcohol, and 34% carboxylic acid groups.
- b. Samples from the SMOG chamber with one-day equivalent oxidation but at lower OM concentrations (which are closer to typical ambient) had an average of 24% alkane, 9% alcohol, and 67% carboxylic acid groups.
3. Comparing the compositions measured by this vehicle testing with atmospheric sampling reveals that PAM and SMOG chamber samples are very similar to vehicle-related emission factors identified in Bakersfield and elsewhere. The low OM in CVS samples is consistent with their small contribution to atmospheric sampling. The substantial contribution of primary amine groups merits further attention.
4. Comparisons to FTIR OFG composition from smog chambers indicate that the PAM and SMOG chamber samples collected here are similar to the secondary OM composition produced by very high oxidant exposures of both

aromatic and alkane pre-cursors. More comprehensive sampling protocols would provide further opportunities for more direct comparisons.

References

Bates, T. S., et al. (2012), Measurements of ocean derived aerosol off the coast of California, *Journal of Geophysical Research-Atmospheres*, 117, 10.1029/2012jd017588.

Corrigan, A. L., et al. (2013), Biogenic and biomass burning organic aerosol in a boreal forest at Hyttiala, Finland, during HUMPPA-COPEC 2010, *Atmospheric Chemistry and Physics*, 13, 12233-12256, 10.5194/acp-13-12233-2013.

Day, D. A., S. Liu, L. M. Russell, and P. J. Ziemann (2010), Organonitrate Group Concentrations in Submicron Particles with High Nitrate and Organic Fractions in Coastal Southern California, *Atmospheric Environment*, 44(16), 1970-1979, 10.1016/j.atmosenv.2010.02.045.

Frossard, A. A., P. M. Shaw, L.M. Russell, J. H. Kroll, M. R. Canagaratna, D. R. Worsnop, P. K. Quinn, T. S. Bates (2011), Springtime Arctic Haze Contributions of Submicron Organic Particles from European and Asian Combustion Sources, *Journal of Geophysical Research*.

Frossard, A. A., L. M. Russell, P. Massoli, T. S. Bates, and P. K. Quinn (2014), Side-by-side comparison of four techniques explains the apparent differences in the organic composition of generated and ambient marine aerosol particles, *Aerosol Science and Technology*, 48, V-X, 10.1080/02786826.2013.879979.

Gilardoni, S., L. M. Russell, A. Sorooshian, R. C. Flagan, J. H. Seinfeld, et al. (2007), Regional Variation of Organic Functional Groups in Aerosol Particles on Four Us East Coast Platforms During the International Consortium for Atmospheric Research on Transport and Transformation 2004 Campaign, *Journal of Geophysical Research-Atmospheres*, 112(D10), 10.1029/2006jd007737.

Gilardoni, S., S. Liu, S. Takahama, L. M. Russell, J. D. Allan, et al. (2009), Characterization of Organic Ambient Aerosol During Mirage 2006 on Three Platforms, *Atmospheric Chemistry and Physics*, 9(15), 5417-5432

Gordon, T. D., Presto, A. A., May, A. A., Nguyen, N. T., Lipsky, E. M., et al. (2014), SOA formation exceeds primary PM emissions for gasoline vehicles, *Atmos. Chem. Phys.*, 14, 4661-4678.

Hamilton, J. F., P. J. Webb, A. C. Lewis, J. R. Hopkins, S. Smith, et al. (2004), Partially Oxidised Organic Components in Urban Aerosol Using Gcxgc-Tof/Ms, *Atmospheric Chemistry and Physics*, 4, 1279-1290.

Hawkins, L. N., and L. M. Russell (2010a), Oxidation of Ketone Groups in Transported Biomass Burning Aerosol from the 2008 Northern California

Lightning Series Fires, Atmospheric Environment, 44, 4142--4154, doi:10.1016/j.atmosenv.2010.07.036.

Hawkins, L. N., and L. M. Russell (2010b), Oxidation of Ketone Groups in Transported Biomass Burning Aerosol from the 2008 Northern California Lightning Series Fires, Atmospheric Environment, 44(34), 4142-4154, 10.1016/j.atmosenv.2010.07.036.

Hawkins, L. N., L. M. Russell, D. S. Covert, P. K. Quinn, and T. S. Bates (2010), Carboxylic Acids, Sulfates, and Organosulfates in Processed Continental Organic Aerosol over the Southeast Pacific Ocean During Vocals-Rex 2008, *Journal of Geophysical Research-Atmospheres*, 115, 10.1029/2009jd013276.

Hayes, P. L., et al. (2013), Organic aerosol composition and sources in Pasadena, California, during the 2010 CalNex campaign, *Journal of Geophysical Research-Atmospheres*, 118, 9233-9257.

Hennigan, C. J., et al. (2011), Chemical and physical transformations of organic aerosol from the photo-oxidation of open biomass burning emissions in an environmental chamber, *Atmos. Chem. Phys.*, 11(15), 7669-7686.

Hildebrandt, L., N. M. Donahue, and S. N. Pandis (2009), High formation of secondary organic aerosol from the photo-oxidation of toluene, *Atmos. Chem. Phys.*, 9(9), 2973-2986.

IPCC (2007), Climate Change 2007: The Physical Science Basis. Contribution of Working Group I to the Fourth Assessment Report 996 pp, Cambridge University Press, Cambridge, UK.

Jimenez, J. L., M. R. Canagaratna, N. M. Donahue, A. S. H. Prevot, Q. Zhang, et al. (2009), Evolution of Organic Aerosols in the Atmosphere, *Science*, 326(5959), 1525-1529, 10.1126/science.1180353.

Kang, E., M. J. Root, D. W. Toohey, and W. H. Brune (2007), Introducing the concept of Potential Aerosol Mass (PAM), *Atmos. Chem. Phys.*, 7(22), 5727-5744.

Kirchstetter, T. W., B. C. Singer, R. A. Harley, G. R. Kendall, and J. M. Hesson (1999), Impact of California Reformulated Gasoline on Motor Vehicle Emissions. 2. Volatile Organic Compound Speciation and Reactivity, *Environmental Science & Technology*, 33(2), 329-336.

Kroll, J. H. and J. H. Seinfeld (2008). Chemistry of secondary organic aerosol: Formation and evolution of low-volatility organics in the atmosphere. *Atmospheric Environment*, 42(16), 3593-3624.

Lambe, A. T., et al. (2011), Characterization of aerosol photooxidation flow reactors: heterogeneous oxidation, secondary organic aerosol formation and cloud condensation nuclei activity measurements, *Atmospheric Measurement Techniques*, 4(3), 445-461.

Li, R., et al. (2015), Modeling the Radical Chemistry in an Oxidation Flow Reactor: Radical Formation and Recycling, Sensitivities, and the OH Exposure Estimation Equation, *J. Phys. Chem. A*, 119(19), 4418-4432.

Liu, S., S. Takahama, L. M. Russell, S. Gilardoni, and D. Baumgardner (2009), Oxygenated Organic Functional Groups and Their Sources in Single and Submicron Organic Particles in Milagro 2006 Campaign, *Atmospheric Chemistry and Physics*, 9(18), 6849-6863

Liu, S., D. A. Day, J. E. Shields, and L. M. Russell (2011), Ozone-Driven Daytime Formation of Secondary Organic Aerosol Containing Carboxylic Acid Groups and Alkane Groups, *Atmospheric Chemistry and Physics*, 11(16), 8321-8341, 10.5194/acp-11-8321-2011.

Liu, S., L. Ahlm, D. A. Day, L. M. Russell, Y. L. Zhao, et al. (2012), Secondary Organic Aerosol Formation from Fossil Fuel Sources Contribute Majority of Summertime Organic Mass at Bakersfield, *Journal of Geophysical Research-Atmospheres*, 117, 10.1029/2012jd018170.

Maria, S. F., L. M. Russell, B. J. Turpin, and R. J. Porcja (2002), Ftir Measurements of Functional Groups and Organic Mass in Aerosol Samples over the Caribbean, *Atmospheric Environment*, 36(33), 5185-5196.

Maria, S. F., L. M. Russell, B. J. Turpin, R. J. Porcja, T. L. Campos, et al. (2003), Source Signatures of Carbon Monoxide and Organic Functional Groups in Asian Pacific Regional Aerosol Characterization Experiment (Ace-Asia) Submicron Aerosol Types, *Journal of Geophysical Research-Atmospheres*, 108(D23), 10.1029/2003jd003703.

Maria, S. F., L. M. Russell, M. K. Gilles, and S. C. B. Myneni (2004), Organic aerosol growth mechanisms and their climate-forcing implications, *Science*, 306, 1921-1924, 10.1126/science.1103491.

Maria, S. F., and L. M. Russell (2005), Organic and inorganic aerosol below-cloud scavenging by suburban New Jersey precipitation, *Environmental Science & Technology*, 39, 4793-4800, 10.1021/es0491679.

May, A. A., et al. (2014), Gas- and particle-phase primary emissions from in-use, on-road gasoline and diesel vehicles, *Atmos. Environ.*, 88, 247-260.

Minguillon, M. C., N. Perron, X. Querol, S. Szidat, S. M. Fahrni, et al. (2011), Fossil Versus Contemporary Sources of Fine Elemental and Organic

Carbonaceous Particulate Matter During the Daure Campaign in Northeast Spain, *Atmospheric Chemistry and Physics*, 11(23), 12067-12084, 10.5194/acp-11-12067-2011.

NRC (1996), A Plan for a Research Program on Aerosol Radiative Forcing and Climate Change, J.H. Seinfeld, R. Charlson, P.A. Durkee, D. Hegg, B.J. Huebert, J. Kiehl, M.P. McCormick, J.A. Ogren, J.E. Penner, V. Ramaswamy, and W.G.N. Slinn, National Research Council, National Academic Press, Washington, D.C.

Petters, M. D., Kreidenweis, S. M., and Ziemann, P. J. (2016), Prediction of cloud condensation nuclei activity for organic compounds using functional group contribution methods, *Geosci. Model Dev.*, 9, 111-124, doi:10.5194/gmd-9-111-2016.

Russell, L. M. (2003), Aerosol Organic-Mass-to-Organic-Carbon Ratio Measurements, *Environmental Science & Technology*, 37(13), 2982-2987, 10.1021/es026123w.

Russell, L. M., R. Bahadur, L. N. Hawkins, J. Allan, D. Baumgardner, et al. (2009a), Organic Aerosol Characterization by Complementary Measurements of Chemical Bonds and Molecular Fragments, *Atmospheric Environment*, 43(38), 6100-6105, 10.1016/j.atmosenv.2009.09.036.

Russell, L. M., S. Takahama, S. Liu, L. N. Hawkins, D. S. Covert, et al. (2009b), Oxygenated Fraction and Mass of Organic Aerosol from Direct Emission and Atmospheric Processing Measured on the R/V Ronald Brown During Texaqs/Gomaccs 2006, *Journal of Geophysical Research-Atmospheres*, 114, 10.1029/2008jd011275.

Russell, L. M., L. N. Hawkins, A. A. Frossard, P. K. Quinn, and T. S. Bates (2010), Carbohydrate-Like Composition of Submicron Atmospheric Particles and Their Production from Ocean Bubble Bursting, *Proceedings of the National Academy of Sciences of the United States of America*, 107(15), 6652-6657, 10.1073/pnas.0908905107.

Russell, L. M., R. Bahadur, and P. J. Ziemann (2011), Identifying organic aerosol sources by comparing functional group composition in chamber and atmospheric particles, *PNAS Early Edition*, 10.1-73/pnas.1006461108.

Schauer, J. J., M. J. Kleeman, G. R. Cass, and B. R. T. Simoneit (1999), Measurement of Emissions from Air Pollution Sources. 2. C-1 through C-30 Organic Compounds from Medium Duty Diesel Trucks, *Environmental Science & Technology*, 33(10), 1578-1587.

Takahama, S., A. Johnson, and L. M. Russell (2013), Quantification of carboxylic and carbonyl functional groups in organic aerosol infrared absorbance

spectra, *Aerosol Science and Technology*, 47, 310-325, 10.1080/02786826.2012.752065.

Tkacik, D. S., et al. (2014), Secondary Organic Aerosol Formation from in-Use Motor Vehicle Emissions Using a Potential Aerosol Mass Reactor, *Environ. Sci. Technol.*, 48(19), 11235-11242.

Weitkamp, E. A., A. M. Sage, J. R. Pierce, N. M. Donahue and A. L. Robinson (2007), Organic Aerosol Formation from Photochemical Oxidation of Diesel Exhaust in a Smog Chamber, *Environmental Science and Technology*, 41(20), 6969-6975.

Zhao, Y., N. T. Nguyen, A. A. Presto, C. J. Hennigan, A. A. May, and A. L. Robinson (2016), Intermediate Volatility Organic Compound Emissions from On-Road Gasoline Vehicles and Small Off-Road Gasoline Engines, *Environ. Sci. Technol.*, 50, 4554-4563.